

Dear Editor and Referees:

Thank you very much for your valuable comments and suggestions concerning our manuscript entitled “Stability evaluation and potential failure process of rock slopes characterized by non-persistent fractures” (ID: nhess-2020-58). These comments are all valuable and helpful for revising and improving our paper, as well as the important guiding significance to our researches. Careful revisions have been made to the manuscript according to the comments and suggestions, which we hope will merit your approval. The revised portions are marked in red in the manuscript. A point-by-point response to your comments and relative changes made in the manuscript are listed as follows.

Responses to Editor

Comment 1: on the basis of the reports of two peer-reviewers, complemented by my own revision of your manuscript, I consider that the content of your research may be of interest for the journal reader and may represent a suitable publication in NHSS should you be ready to incorporate some major revisions.

Response: Thank you very much for your positive evaluation. We have revised our manuscript carefully according to all comments and the revised portions are marked in red in the revised manuscript. We sincerely hope our revised paper will merit your approval.

Comment 2: Please carefully look at all the comments and remarks made by the two referees and reply to them, one by one. Where required, please modify the original manuscript and provide a new amended copy along with the document with replies to the reviews.

Response: Thank you very much for your comment. We have carefully looked at and replied to all comments and suggestions one by one, which can be found in Responses to Referee #1 and Responses to Referee #2. In addition, the previous manuscript have been modified according to these comments and suggestions, which can be found in the relative responses as well as the revised manuscript.

Comment 3: In particular, I am concerned about the main issue that is raised by Reviewer #2 on

the model adopted to represent the rock mass and the fracture network. I agree with the reviewer that such DFN representation, despite being suitable in terms of conceptual model representation, does not seem suitable for the representation of the actual rock mass, where the role of the small fracture sub-network cannot be overlooked without compromising the entire numerical description of the whole.

Response: Thank you very much for your comment. It is really true that the role of the small fractures cannot be overlooked in the stability analysis. DFNs in the previous manuscript only consider the fractures with trace lengths larger than 1.5 m, which indeed overestimate the stability of the rock slope. In the revised manuscript, we accepted the suggestion of Referee #2, i.e., decreasing the strength of intact rock materials to account for the small fractures that are not implemented as discrete discontinuities in the DFN. The new numerical results demonstrated that the new safety of factors (12-38) were lower than the previous ones (25-73.5), while the critical slip surface and potential failure process remained the same as the previous ones. Relative changes in the revised manuscript have listed in the responses to Referee #2 and therefore are not described in detail in this place.

Comment 4: Also, please consider the remarks of reviewer #1, with specific reference to the one related to the choice of the slope for the numerical analysis, which is quite stable and not prone to failure. That leaves no room to variability in slope behaviour and seems to underestimate the scope of the work. Again, this issue could be related to the previous one as raised by reviewer #2.

Response: Thank you very much for your comment. The comprehensive method we proposed aims to analyse the stability of rock slopes characterized by non-persistent fractures. Therefore, we selected a slope whose stability is completely controlled by non-persistent fractures. However, the safety factors of this type of slopes are always high (more than 10) due to the high strength of rock bridges (Huang et al., 2015). Although the slope we analysed is quite stable and failure hardly occur in the future, we believe the proposed method really make sense for engineering projects related to fractured rock slopes.

Comment 5: Please also consider all remaining remarks and minor requested made by the two referees, as in the attached material. I am confident that, after considering all the previous points,

your manuscript will be in a form which will be of great interest for the journal readers.

Response: Thank you very much for your suggestion. We have looked at all comments and remarks made by the two referees one by one and modified our manuscript based on these comments and remarks. The revised portions are marked in red in the revised manuscript. Meanwhile, relative revisions are also listed in the corresponding responses to Referee #1 and Referee #2.

We tried our best to improve and make changes to the manuscript. We sincerely appreciate your work and hope that our revised manuscript will be met with approval. Once again, thank you very much for your favorable comments and suggestions!

Relevant references:

Huang, D., Cen, D. F., Ma, G. W., and Huang, R. Q.: Step-path failure of rock slopes with intermittent joints, *Landslides*, 12, 911–926, 2015.

Responses to Referee #1

Comment 1: L 69-70: Authors state: “These slopes may become hidden dangers (e.g., geological disasters) and pose potential threats to people and nearby equipment”. This sentence is in strong contrast with the results from the stability analyses, since the safety factors range from 25 to 75. I’m wondering if the investigated slope is really too stable or the safety factors could have been somehow overestimated. Nevertheless, no event seems to have occurred in recent times from the investigated slope; this is a pity, since real events could have been extremely useful for validating the performed analyses. Why did Authors choose to test the proposed procedure to this slope?

Response: Thank you very much for your comment. It is really true that the investigated slope is stable according to its safety factors; thus, a large-scale rock slide can hardly occur. Only some small-scale rock falls may happen. Therefore, we corrected this sentences as “These slopes may become rock falls and pose potential threats to people and nearby equipment. Whether rock slide will happen requires calculating and evaluating”. (Page 3: Lines 71-73 in the revised manuscript)

The investigated rock slope is highly stable according to the following reasons: 1) weak interlayers and through-going discontinuities are not developed in the field; 2) the amount of rock

bridges along the slip surface is about 30%-40%, which will stabilize the slope because the rock bridges are multiple orders of magnitude stronger than fractures.

It is really a pity since no real event can be used for validating the performed analyses. We have investigated many destroyed slopes. The results shown that the stabilities of the slopes are always controlled by weak interlayers or through-going discontinuities. This type of slopes is disadvantageous to our analysis of the influence of non-persistent fractures on rock slope stability. Therefore, we selected a slope whose stability is completely controlled by non-persistent fractures. However, the safety factors of this type of slopes are always high (more than 10) (Huang et al., 2015). In the revised manuscript, we decreased the strength of the intact rock materials according to equivalent strength of equivalent rock mass. The new modeling results showed the factors of safety remains high (from 12 to 38) but lower than the previous ones (from 25 to 73.5). We will select the rock slope with more fractures to test the proposed method for future researches. Nevertheless, we believe the proposed method really make sense for engineering projects related to fractured rock slopes.

Comment 2: L 92-93 and figure 3: the division of the detected discontinuities into sets is rather questionable, since data dispersion is indeed too high. Yet, this should not affect model reconstruction too much, as dispersion is also considered in the generation of artificial discontinuities within the DFN model.

Response: Thank you very much for your comment. It is really true that the data dispersion is high. An important reason of this phenomenon is that small-scale structural fractures with highly dispersed orientations predominate in the exposed rock surface. Subsequently, some fracture poles are also dispersed for each set. However, the distances between these fracture poles and the centre of the set is indeed closer compared with that between them and the other two sets, which was validated using the method proposed by Chen et.al (2005). Therefore, the grouping results are reasonable.

It is really true as you said that the data dispersion is high, but it is not caused by grouping. Even though fractures with similar orientations are divided into one set, the orientations of fractures in the same set still present dispersion to some extent.

We considered the dispersion of all fracture orientations in the field. The final DFN model is formed by combining three fracture sets. Therefore, the data dispersion will not affect the establishment of the DFN model.

Comment 3: L184: I suggest not to take for granted what a “fish function” is; please explain for those unfamiliar with numerical modelling.

Response: Thank you very much for your suggestion. It is really true that fish function may be hard to be understood for those unfamiliar with numerical modelling. Therefore, “fish function” was interpreted in the revised manuscript as “Then, an embedded scripting language in PFC, i.e., FISH, is used to write user-defined functions for extending the functionality or adding user-defined features in PFC. In the present study, we used the FISH functions to add the DFN into the model of the slope section by reading the location data of fractures. Subsequently, the SRM model composed of the BPM and DFN is established”. (Page 8: Lines 231-234)

Comment 4: L255-259: The modelling results are nice and look quite reasonable, but without validation they seem to be an end into themselves. Did any real event occur from the investigated slope in recent times? Are there any detached blocks to compare their volume and shapes with the simulated ones? What about their runout? In my opinion the reliability of the proposed procedure needs to be demonstrated.

Response: Thank you very much for your positive feedback of the modelling results. No rock slide has occurred in recent times from the investigated slope, which is clearly confirmed by the high factors of safety computed in the simulations; thus, it is hard to compare the volume and shapes of the real and simulated ones. It is really a pity since no real event can be used for validating the proposed procedure. We will select the rock slope with more fractures to test the proposed method for future researches.

Comment 5: L260: Please change section 6 title, since “stability analysis” has already been used for section 4. Maybe, “Statistical analysis”?

Response: We are very sorry for our carelessness. It is really true that the title of section 6 should be “Statistical analysis”. In the revised manuscript, the title of section 6 has been changed to “Statistical analysis”. (Page 10: Line 311)

Comment 6: L281: please change are 43.5 to is 43.5

Response: We are very sorry for our improper word. In the revised manuscript, we changed “are” to “is” (Page 11: Line 332). In addition, we carefully checked the revised manuscript to ensure that all vocabulary and grammar errors were corrected.

Comment 7: L327 and 334: To trigger instability, Authors used the gravity increase method proposed by Meng et al. (2015). It is not clear to me if Authors made some amendments to this method, or if they used it as is. If so, in my opinion, the method cannot be defined as “innovative”.

Response: Thank you very much for your suggestion. In the present research, we directly applied the improved gravity increase method proposed by Meng et al. (2015) to trigger instability. We are very sorry for our wrong use of the word “innovative”. Although this method is relatively new compared with traditional gravity increase method, this study cannot refer this approach as an innovative one. Therefore, we deleted the word “innovative” and rewrote this sentence as “The factor of safety is determined on the basis of the improved gravity increase method”. (Page 12: Lines 377-378)

Comment 8: Figure 1: Fig 1b: image is not clear; I suggest deleting the text superimposed over the image. Fig 1c: if the image contains the window reported in Figure 2, please add the box limits.

Response: Thank you very much for your suggestion. In the revised manuscript, we deleted the text superimposed over the image in Fig. 1b as you suggested. In addition, we enhanced the contrast to improve the image clarity. (Page 17: Figure 1b)

It is really true that Fig. 1c contains the window reported in Fig. 2; thus, as you suggested, we added the box limits corresponding to the sampling window in Fig. 1c. (Page 17: Figure 1c)

Comment 9: Figure 7 In my opinion, the picture in picture representation is misleading. If possible, add all the drawings in a single image, otherwise, split in two different figures.

Response: Thank you very much for your suggestion. It is really true that one image composed of two pictures is misleading. In the revised manuscript, we added all drawings in a single image. In addition, we added detailed description in the caption of Fig. 7, which would help further understand the meaning of each image. (Page 20: Figure 7)

Comment 10: Figure 8: to improve image resolution, I suggest cropping the images to the

fractured sectors.

Response: Thank you very much for your suggestion. It is really true that the resolution of Fig.8 is low. In the revised manuscript, the boundary sector without fractures were cropped and only remained the fractured sectors to improve image resolution. (Page 21: Figure 8)

Comment 11: Figure 9: sometimes the timestep count is represented in decimal notation and sometimes in scientific notation, please uniform.

Response: Thank you very much for your suggestion. It is really true that the expression of the timestep count should be uniformed. In the revised manuscript, we changed the timestep count represented in decimal notation to scientific notation. Specifically, 2000, 5000, 10000, 20000, 40000, 60000, and 80000 were changed into 2×10^3 , 5×10^3 , 10^4 , 2×10^4 , 4×10^4 , 6×10^4 , and 8×10^4 , respectively. (Page 20: Figure 7; Page 21: Figure 8)

We thank you for your valuable comments and suggestions. These comments are all valuable and helpful in revising and improving our paper, as well as in guiding the significance of our research.

Relevant references:

Chen, J. P., Shi, B. F., and Wang, Q.: Study on the dominant orientations of random fractures of fractured rock mass, Chinese Journal of Rock Mechanics and Engineering, 24, 241–245, 2005.

Huang, D., Cen, D. F., Ma, G. W., and Huang, R. Q.: Step-path failure of rock slopes with intermittent joints, Landslides, 12, 911–926, 2015.

Meng, Y. D., Su, Q. M., Lu, W. P., and Xu, Z.: Research on improved grain flow gravity increase method, Chinese Journal of Water Resource and Power, 33, 149–151, 2015.

Responses to Referee #2

Comment 1: The first general comment is that the investigated slope is quite low (20 m in the simulated models). It is true that in certain conditions brittle damage can develop even in low stress conditions, especially when tensile strength is exceeded or in case of significant stress

concentrations. However, in this case it seems that the amount of rock bridges along the critical path(s), would most likely stabilize the slope, except perhaps for small blocks at surface. It is very unlikely that the real slopes will ever fail with the simulated mechanism, unless smaller fractures are included in both the data collection and DFN. This is clearly confirmed by the high factors of safety computed in the simulations.

This brings me to the second, important comment: the model input data, which seems the “weak point” of this manuscript. It is not clear what technique was used for the initial data collection, but the DFN used in the models seems to rely on and include only the larger discontinuities. This results obvious by visually comparing figure 1c and figure 2 (which seems to depict a much more fractured rock mass). Considering the input DFN, the high factors of safety computed makes sense. However, the question is: “is this DFN a realistic representation of the real rock mass?”. The issue with the input data may have significantly impacted the numerical results, in terms of factor of safety, and location of the critical path. A “work around” would be to decrease the simulated strength of the intact material, to account for the smaller fractures that are not implemented as discrete discontinuities in the DFN.

In conclusion, in its present form, the manuscript seems quite conceptual, in that there is a seemingly weak connection between the model and the actual rock mass. While the simulations may indeed reproduce a realistic fracture propagation mechanism, the actual process is very unlikely to occur in the simulated slope, or any slope with similar height, lithology, and structural configuration. In view of this, this paper should be significantly improved (major revisions) with regard to the model input data and their description. Either by a) including the fractures that seem to be missing in the DFN, or b) demonstrating in a clearer manner the similarity between the DFN and the rock mass. This could include better pictures, with close-ups and, importantly, scales. Showing the mapped traces onto the photo of the slope could also greatly improve the clarity.

[Response:](#) Thank you very much for your comment. It is really true that the investigated slope can hardly fail considering the low height, a large amount of rock bridges along the slip surface. This is also confirmed by the high factors of safety. When it is subjected to significant environmental changes, such as earthquakes, rainfall, unloading, or overloading, the failure may occur following

the potential failure mechanism.

The sampling window method (Kulatilake and Wu 1984) is used to collect fracture data in the present study. It is really true that the generated DFNs rely on and include the larger fractures since only fractures with the length larger than 1.5 m were measured in the field. The amount of fracture with the length smaller than 1.5 m are extremely large, which goes beyond the artificial measurement. Considering that small fractures have a little effect on slope stability, we take the cut-off limit of 1.5 m.

On the basis of the collected fracture data in the exposed rock surface, the DFN is a most possible representation of the real rock mass. However, it is really true that the DFN is more accurate and the numerical results are more reasonable if smaller fractures are taken into consideration. In the revised manuscript, we decreased the strength of the intact material to remedy the lack of smaller fractures in DFN. Specifically, particle parameters which influence the strength of intact material, including the friction coefficient of particles, tensile strength of parallel bond, and cohesion of parallel bond are synchronously reduced by half according to the equivalent shear strength of equivalent rock mass.

The new modelling results demonstrated that the factors of safety are lower when the strength of intact rock material than the previous ones, indicating the lack of smaller fractures indeed makes the factors of safety relatively high. Even so, the factors of safety remain high, which are between 12 and 38. In addition, the location of the critical slip surface remains the same as the previous one since the slip surface is always composed of pre-existing fractures and new-propagated ones. Similarly, the potential failure process is roughly identical to that of previous simulation since both are conducted in the natural condition (i.e., the gravity acceleration is 10.0).

In the revised manuscript, corresponding content of parameter reduction and the new modelling results are rewrote. Details can be found in Lines 90-92 and 176-204 in the revised manuscript, which are also listed in the end of this response. In addition, the scales were added in all required figures and the location of the mapping window has been added in Fig. 1c. We also carefully checked the whole manuscript and considered all of your line-by-line comments.

Page 3: Lines 90-92: “Fractures in the exposed surface with trace lengths smaller than 1.5 m are widely distributed and difficult to record. Therefore, these fracture are not considered when performing fracture data collection for 2D DFN simulation. Nevertheless, the effect of these fractures on the rock mass strength is considered, which is explained in Sect. 3.1”.

Pages 6-7: Lines 176-204: “It should be noted that parameters in Table 2 are representations of intact rock materials in PFC2D. However, fractures with trace lengths smaller than 1.5 m were disregarded in the collection of fracture data, but these clearly represent a weakness. Considering the effect of these fractures on strength of the intact rock material make a significant difference to the following stability analysis. In the present study, the combination of intact rock mass and these small fractures is considered as the equivalent rock mass. Obtaining the equivalent shear strength of the equivalent rock mass is extremely important since the rock mass failure is generally promoted by the reduction of the shear strength of rock mass (i.e., the shear strength reduction method). An equivalent shear strength calculation was developed based on the Mohr-Coulomb criterion (Lajtai, 1969b; Shang et al., 2018), as expressed by the following equation:

$$\tau = c_e + \sigma \tan \varphi_e = [K_L \cdot c_f + (1 - K_L) \cdot c_R] + \sigma [K_L \cdot \tan \varphi_f + (1 - K_L) \cdot \tan \varphi_R] \quad (1)$$

where τ and σ represent equivalent shear strength of the equivalent rock mass and normal stress; c_e and φ_e are the equivalent cohesion and friction angle of equivalent rock mass; c_f and φ_f are the cohesion and friction angle of fractures; c_R and φ_R are the cohesion and friction angle of intact rock mass; K_L is the linear persistence.

The values of c_R , φ_R and φ_f are 12.25, 25, and 18, which are listed in Tables 2 and 3. Filed investigation demonstrated that no fillings existed in fractures, implying the cohesion of fractures is equal to zero (i.e., $c_f = 0$). The linear persistence is defined as the ratio of fracture trace lengths and the total length of coplanar given line (Shang et al., 2018; Zhang et al., 2020b). In the present study, several lines with different directions are set in the exposed surface and then the linear persistence is measured. The average linear persistence is considered as the final linear persistence of the equivalent rock mass, whose value is around 50%. Subsequently, substituting aforementioned parameters into Eq. (1), we can deduce that the shear strength of the equivalent rock mass is slightly larger than half of intact rock mass. Nevertheless, Eq. (1) tends to

overestimate the shear strength of equivalent rock mass; thus, the shear strength of the equivalent rock mass is assumed as half of intact rock mass. This assumption is beneficial to the equivalent reduction of relative parameters of intact rock mass in PFC2D; simultaneously, a smaller strength of equivalent rock mass contributes to a relatively small factor of safety, which is more conservative and favourable for engineering projects.

The shear strength of rock materials is controlled by three parameters (including tensile strength of parallel bond, cohesion of parallel bond and friction coefficient of particles) in PFC2D (Bonilla-Sierra et al., 2015). Therefore, these three parameters are synchronously reduced by half while other parameters are kept constant. Specifically, the values of the tensile strength and cohesion of parallel bond and friction coefficient of particles are 12.5MPa, 12.5MPa and 0.35, respectively. By this way, the effect of small fractures are considered in the generation of intact rock mass. Equivalent parameters of the equivalent rock material are obtained and adopted in the generation of SRM model.”

Notably, the contents of critical slip surface and potential failure process are not modified because they are the same as the previous ones. The only difference is that the values of factors of safety and thus only this portion is changed.

Comment 2: Line 40: authors should refer to “the non-persistent fractures in these works”, rather than “these non-persistent fractures”.

Response: Thank you very much for your correction. In the revised manuscript, we have changed “these non-persistent fractures” to “the non-persistent fractures in these works”. (Page 2: Line 40)

Comment 3: Line 51: SRM has been used also for underground applications, including mining and hydraulic fracturing.

Response: Thank you very much for your comment. We carefully searched the literatures regarding underground applications of SRM approach. It is really true that SRM approach has been widely used in mining and hydraulic fracturing. Therefore, we added corresponding description as “SRM models have been primarily used to simulate failure and deformation of fractured rock slopes (Bonilla-Sierra et al., 2015; Elmo et al., 2013), simulate hydraulic fracturing in naturally fractured reservoirs (Damjanac and Cundall, 2016), and estimate rock mass strength,

fragmentation and micro seismicity in caving mines (Lorig et al., 2017)”. (Page 2: Lines 50-53)

Comment 4: Lines 51-53: perhaps these two sentences can be merged. However, the first sentence requires rephrasing, as it seems some words are missing.

Response: Thank you very much for your suggestion. The latter sentence is the explanation of the former one; thus, these two sentences can indeed be merged. In the revised manuscript, we merged the two sentences as “DFN simulation included in SRM modeling program presents a significant variability, which means numerous possible realizations of 2D fracture systems exist given specified input parameters (Pine et al., 2006; Zhang et al., 2020a)”. (Page 2: Lines 53-55)

Comment 5: Line 58: authors should state the country the investigated site is located in.

Response: Thank you very much for your suggestion. In the revised manuscript, we stated the country the investigated site is located in and described as “This study proposes a comprehensive approach that combines several well-established methods to conduct a stability evaluation and failure process analysis of a fractured rock slope in Tianjin City, China.” (Page 2: Line 61)

Comment 6: Line 71-72: this sentence can be improved. Perhaps the slopes are higher to the south, rather than the quarry area itself. Also, from this sentence it is not clear whether the “mountain “is a ridge oriented north-south, or the if the bedding are dipping to north (or south).

Response: We are very sorry for our unclear description. Actually, all sentences from Line 71 to 73 contribute to the description of the study area (i.e., the quarry area). Therefore, it is true that the quarry area is higher in the north. The “mountain” in this place refers to the monoclinical mountains striking south-north. In the revised manuscript, we rewrote these sentences as “The Laohuding Quarry area is characterized by the low-mountain terrain, which is higher in the north than in the south. The highest and lowest altitudes of the quarry area are 160 m and 60 m, with a relative elevation of 100 m. A majority of monoclinical mountains striking south–north exist in this area. The average slopes of the mountains in the east and west of the quarry area are 25 ° and 30 °, respectively (Fig. 1b)”. (Page 3: Lines 74-77)

Comment 7: Line 79: is the formation thick, or the limestone layers? Either way, how thick? Karst phenomena are not obvious, meaning there is not any, or that they are not or scarcely visible?

Response: We are very sorry for unclear description. Actually, we initially aims to say “The

limestone is moderately weathered” rather than “The limestone is moderately thick”. In the revised manuscript, we corrected it. (Page 3: Line 83) “the karst phenomena are not obvious” means that the karst phenomena are scarcely visible in the study area due to low precipitation and the lack of groundwater. In the revised manuscript, we rewrote this sentence as “the karst phenomena are scarcely visible due to low precipitation and groundwater shortage.” (Page 3: Lines 83-84)

Comment 8: Lines 80-83: the last two sentences could be merged. The term “intermittent” for discontinuities is somewhat inaccurate (or simply very rarely used, to my knowledge) – perhaps simply “non-persistent” is more appropriate. Additionally, one would expect that bedding would be very persistent. Will this play a role? Although it is true that observing the bedding trace does not necessarily imply a fully persistent plane with no tensile strength.

Response: Thank you very much for your suggestion. It is really true that the term “intermittent” for discontinuities is rarely used. In the revised manuscript, we used “non-persistent” to substitute it as you suggested. (Page 3: Line 85) Field observation demonstrated that no bedding planes, faults, folds, and shear zones are developed in the rock exposure. Therefore, the bedding plays no role in stability analysis. It is non-persistent fractures that play the most significant role in the slope stability and potential failure process. Aforementioned descriptions are rewrote in the revised manuscript as “Faults, folds, bedding planes, shear zones and weak interlayers are not observed, and thus, this area is tectonically stable. Non-persistent discontinuities are randomly and widely developed in outcrops (Fig. 1c). Therefore, it is the non-persistent discontinuities (fractures) that control the slope stability and potential failure process”. (Page 3: Lines 84-87)

Comment 9: Line 86-92: A 62 by 6 m is a large area to perform systematic discontinuity mapping (i.e. using traditional field techniques or short range remote sensing methods), and 169 discontinuities seems a low figure – what is the cut-off limit you considered (i.e. the smallest fracture that was considered). Looking at figure 2, it seems that the location of the mapped discontinuities is slightly biased towards the bottom of the window. Because of this, I would assume that the mapping was performed using traditional field methods, rather than remote sensing techniques. Either way, this should be mentioned, also to address or acknowledge the

potential limitations of the methodology used, in terms, for instance, of orientation bias. Speaking of orientation bias, the fracture set 1 is suggested to be less represented – this might be due to its orientation very similar to the slope, while sets 2 and 3 are almost perpendicular. It is not clear whether this was kept into account.

Response: Thank you very much for your suggestion. When collecting fracture data in the field, the cut-off limit we considered is 1.5 m. The reason we chose this cut-off limit is that the amount of fractures with the length smaller than 1.5 m are quite large, which is beyond the artificial measurement; besides, the effect of small fractures on the slope stability is comparatively smaller than big ones. According to the cut-off limit, the number of eligible fractures is exactly 169 in the sampling window.

We are sorry for not mentioning the method we used for collecting fractures. Your assumption is right that the traditional field method, i.e., the sampling window method (Kulatilake and Wu, 1984) is used to collect fractures. The sampling window method mainly presents two limitations: 1) orientation bias and 2) trace length bias. Orientation bias occurs because the probability that fractures with small intersection angles between the fractures and exposed rock surface can be collected in the field is smaller than those fractures with large angles. In our work, the fractures were divided into three sets, namely, fractures of sets 1, 2, and 3 with average orientations of $39.5^{\circ}/87.3^{\circ}$ (dip direction/dip angle), $307.4^{\circ}/44.7^{\circ}$, and $110.2^{\circ}/31.7^{\circ}$, respectively. The strikes of sets 2 and 3 are similar and almost 90 degrees apart from that of set 1. The modelled section, i.e., the cross section, is normal to the exposed rock surface, indicating the strike of it is 110 degrees and is similar to that of set 1 (The strike and dip direction are 90 degrees apart). Therefore, a substantial portion of the fractures of set 1 are not be used in the simulation of 2D DFN models and in the following stability analysis.

Trace length are biased due to two conditions: 1) only one end of a fracture is measured and (2) no end of a fracture is measured. In the present study, we corrected the trace length data using the method introduced by Kulatilake and Wu (1984). Table 1 lists the mean value and probability density function (PDF) of the corrected trace lengths for each fracture set.

In the revised manuscript, we mentioned the sampling window method and the limits of it as

“The characteristics (such as orientation, trace length, spacing, roughness, aperture, filling, and termination) of fractures with trace lengths larger than 1.5 m were systematically surveyed using the sampling window method (Kulatilake and Wu, 1984)” (Page 3: Lines 92-94), “The sampling window method features two main limits of orientation bias and trace length bias. The measured trace lengths bias occurs due to the following: (a) only one end of a fracture is measured, (b) both ends of a fracture are measured, and (c) no end of a fracture is measured” (Page 4: Lines 103-105), and “Orientation bias occurs because the fractures with small intersection angles between the fractures and exposed rock surface are more possibly collected in the field than those fractures with large angles. In the present study, the cross section normal to the exposed surface was used to perform the 2D stability analysis. The dip directions of fractures in set 1 are similar to that of the cross section, implying fractures acted as the surface of separation, which will not influence the results of stability analysis. Therefore, a substantial portion of the fractures of set 1 (fractures intersected by the cross section with an angle smaller than 20 °) were artificially deleted prior to the stability analysis”. (Page 4: Lines 107-113)

Comment 10: Line 90: Reference here seems out of place, unless the result came from that specific work.

Response: Thank you very much for your suggestion. The reference aims to present that the grouping method used in the present study is suggested by it. It is really true that the reference should not be put in this place. In the revised manuscript, we put the reference in the right place by rewriting the sentence as “The fractures can be divided into three sets using the method proposed by Chen et al. (2005), as shown in Figure 3”. (Page 4: Lines 98-99)

Comment 11: Line 94-95: This sentence requires rephrasing. I suggest starting from the issue of the trace length bias, and then stating the reason, rather than the contrary.

Response: Thank you very much for your suggestion. We accept your professional suggestion and rewrote this sentence as “The sampling window method features two main limits of orientation bias and trace length bias. The measured trace lengths bias occurs due to the following: (a) only one end of a fracture is measured, (b) both ends of a fracture are measured, and (c) no end of a fracture is measured”. (Page 4: Line 103-105)

Comment 12: Line 99: I recommend “and ‘investigate the’ potential failure mechanism”.

Response: Thank you very much for your suggestion. In the revised manuscript, we rewrote this sentence as you suggested, i.e., “The cross section normal to the exposed surface was used to perform the 2D stability analysis and investigate the potential failure mechanism of the rock slope”. (Page 4: Lines 109-110)

Comment 13: Lines 105-107: It seems the authors suggest that the fracture intensity in a section is a function of the orientation of the set, with respect to the north. This is a bit counter-intuitive, as the orientation of the rock face (and specifically the angle with the fracture set) is surely more relevant than the azimuth (angle with the North) of the fracture – which in fact should not be that important. More detail on the method should be provided to improve clarity.

Response: We are sorry for our unclear description. The slope is oriented at a trend of 200 °, we rotated the slope 20 ° so that the slope exactly strikes in the NS direction prior to the deduction of the function. The information above is omitted in our paper considering it has been explained in the work of Zhang et al. (2017). However, the omission of this important information obviously results in the misunderstanding. In the revised manuscript, we added this information and interpreted this function as “We rotate the slope 20° so that the slope strikes in the NS direction and assume the fracture frequency measured along the mean normal vector direction of fracture set i is λ_i , and the acute angle between this direction and NS direction is η_i . The fracture frequency along the line parallel to the strike of the outcrop plane is $\lambda_i \cos \eta_i$ (Priest 1993), and the cross section plane is $\lambda_i \sin \eta_i$. The fracture frequency of the latter is $\tan \eta_i$ times that of the former, and P_{21} (2D fracture intensity) follows this result according to the concept of the integral”. (Page 4: Lines 118-122)

Comment 14: Line 106: P_{21} is “fracture intensity”, not “fracture density” (which is P_{20} in the 2D case).

Response: We are sorry for our wrong use of the term “fracture density”. It is really true that P_{21} is fracture intensity, which represents the length of fractures per unit area of rock mass (m/m^2). P_{20} is fracture density, which describes the number of fractures per unit area of rock mass (m^{-2}). In the revised manuscript, we changed “2D fracture density” to “2D fracture intensity”. (Page 4: Lines

121-122)

Comment 15: Line 117-118: The second statement seems to suggest that different input data (“fracture characteristics”) were used for the four DFN realizations.

Response: We are sorry for our unclear description. “Input fracture data” is different from “fracture characteristics” in our description. The former one refers to indispensably statistical fracture data for establishing the DFN, such as the distribution types of fracture locations, P_{21} , the mean and variance values of the trace lengths. A majority of DFNs can be generated by Monte Carlo simulation on the basis of these statistical fracture data. Therefore, input data are the same for different DFNs, which explains the first sentence “More than one DFN can be generated with the same fracture data”.

The latter one represents the specific fracture characteristics that the generated DFMs present, such as the specific location, dip angle, and trace length of each fracture. These fracture characteristics vary for different DFNs, which is described in the second sentence, i.e., “For example, Fig. 4 exhibits four DFNs with different fracture characteristics”.

It is really true that the statements of the two sentences are misleading according to your comment; thus, we rewrote the two sentences in the revised manuscript as “More than one DFN can be generated on the basis of the aforementioned statistical fracture data. For example, Fig. 4 exhibits four DFNs with the same statistical fracture data, but fracture characteristics, such as locations, dip angles, trace lengths, are different from one another”. (Page 5: Lines 132-134)

Comment 16: Lines 120-123: Perhaps a sketch would help the reader understanding the procedure. Also, I believe this procedure is performed in 2D. If so, I suggest to use slope “profile” instead of “surface” – this would make the procedure easier to understand for the reader (especially if no figure is provided).

Response: Thank you very much for your suggestion. It is really true that the procedure is performed in 2D. We are sorry for the wrong use of “surface”. In the revised manuscript, we changed “the exposed surface” to “lines extending along the dip direction of the cross section”. (Page 5: Lines 138)

Comment 17: Line 130: even more importantly, SRM is used to simulate the brittle propagation of

fractures, and thus the brittle behavior of rock masses.

Response: Thank you very much for your comment. It is really true that SRM is widely used to simulate the brittle propagation of fractures, which we mentioned in Introduction but ignored here. In the revised manuscript, we added this application and described as “SRM approach is widely used to reproduce the mechanical properties and behaviours of fractured rock masses, simulate the fracture propagation and brittle failure of fractured rock masses, and perform stability analysis of fractured rock slopes”. (Page 5: Lines 146-148)

Comment 18: Line 134: it would be good to provide a couple of examples (even in brackets) of the micro-properties that are used as input.

Response: Thank you very much for your suggestion. It is indeed better to provide some examples of the input micro-properties first. In the revised manuscript, we added some examples of micro-properties as “The SRM model in PFC2D is defined by many parameters, such as particle contact modulus, particle normal/shear stiffness ratio, and parallel bond modulus. These parameters cannot be directly identified via laboratory and field experiments”. (Page 5: Lines 150-151)

Comment 19: Line 160: perhaps “interpenetrate” or “compenetrate” is a better term than “pass through”.

Response: Thank you very much for your suggestion. The word “interpenetrate” is indeed much better than “pass through”; thus, we replaced “pass though” with “interpenetrate” in the revised manuscript. (Page 7: Line 206)

Comment 20: Lines 186-188: this assumption is perhaps more adequate considering the low stress conditions that characterize the real slope.

Response: Thank you very much for your suggestion. It is really true that the investigated slope is characterized by low stress conditions; thus, we added this reason as the support of the assumption in the revised manuscript. Specifically, it is described as “This process ignored the stress concentration at the tips of the structural fractures generated by tectonic stress, which was considered reasonable in this study since the investigated slope is characterized by the low stress conditions and the stress concentration was intensely reduced after the long-term stability of the

rock slope”. (Page 8: Lines 235-238)

Comment 21: Line 190: Just a comment here. As the authors know, this approach may be “risky” in other conditions (i.e., high stress/high slopes) as it may cause a “shock” in the model, causing excessive damage in the slope, compared to a progressive excavation (or a progressive removal of the boundary), which generally is more representative of a “real world” situation.

Response: Thank you very much for your comment. It is really true this approach (one- time removal of the boundary) may cause excessive damage in the slope, especially for high slopes. However, the investigated slope was exactly formed by one excavation in the real condition; thus, the approach, i.e., one-time removal of the boundary, is practical. As for other high slopes, which may be more likely to be formed by progressive excavations, the progressive removal of the boundary is more appropriate. The specific approach to removing the boundary should be determined according to excavation methods of slopes.

Comment 22: Lines 194-197: It is unclear what are the benefits of decreasing the friction coefficient while increasing gravity. Intuitively, the gravity increase already would induce an increase in shear stresses compared to the initial state (very much like increasing the density). How is this double effect (increase in shear stress, decrease in shear strength) accounted for in the FoS calculation? And why just the friction, and not the cohesion? The paper would benefit from a more detailed explanation of the method employed.

Response: We are sorry for our unclear description. It is really true that the increase of gravity would induce the increase in shear stress, as well as the increase in normal stress. The increases in both stresses lead to increases in driving and resisting forces, which makes the change in factor of safety unclear. Therefore, the factor of safety cannot be reflected by only increasing the gravity. Only if one of the forces (driving or resisting forces) is fixed can the change of the other be related to the factor of safety. The driving force cannot be fixed because it is directly proportional to gravity; thus, the resisting force should be fixed. The resisting force is directly proportional to the shear strength, which is equal to $c + \sigma \tan \varphi$ (where c is cohesion; σ is the normal stress, and φ is friction angle). σ increases when the gravity increase; thus, $\tan \varphi$ is considered to be reduced for making resisting force constant. In PFC, $\tan \varphi$ is directly proportional to the friction coefficient of

particle; thus, the decrease of the friction coefficient of particle can lead to the decrease of $\tan \phi$. In addition, the friction coefficient has little influence on cohesion; thus, making the amplitude of reduction of the friction coefficient is the same as that of the increase in gravity acceleration can ensure an approximate invariance of the resisting force. It is followed that the factor of safety is the ratio of the gravity acceleration in the limit equilibrium state (g') to that in the initial state (g), i.e., $F = g' / g$.

The details above are not described in the previous manuscript, which is indeed hard to tell the benefits of the method. In the revised manuscript, we further interpreted the improved gravity increase method as “This method leads to the failure of a slope in PFC2D by slowly increasing gravity acceleration and reducing the friction coefficient of particles while keeping other parameters constant. Notably, the amplitude of reduction of the friction coefficient is the same as that of the increase in gravity acceleration. In this way, the resisting force can be fixed and therefore the factor of safety is directly reflected by the driving force”. (Page 8: Lines 244-247)

Comment 23: Line 202: this seems a very stable slope. Expectedly, in view of the amount of rock bridges along the rupture surface, which may be estimated at about 30-40%, according to figure 7.

Response: Thank you very much for your comment. It is really true that the investigated rock slope is extremely stable, which can be reflected by the high factors of safety. As you said, the amount of rock bridges along the rupture surface can also verify that the investigated slope is very stable.

Comment 24: Line 232 (and after): Perhaps it will be better to refer to the “slip mass” as “failed”, or “detached” mass/volume/material.

Response: Thank you very much for your suggestion. It is really true that “failed mass” is better than “slip mass”; thus, we carefully checked all the manuscript and changed “slip mass” to “failed mass”. (Page 9: Lines 282-283, 284; Page 10: Lines 288-289; Page 11: Lines 327-328)

Comment 25: Line 255: I recommend referring to the “model geometry” or “morphology”, rather than “shape”.

Response: Thank you very much for your suggestion. It is really true that “morphology” is better than “shape”. We replaced “shape” with “morphology” in the revised manuscript. (Page 10: Line

306)

Comment 26: Line 272: A variability 25-75 is indeed very high. Perhaps this variability be lower if a more realistic DFN (i.e. inclusive of smaller fractures) was to be simulated. Absolute values would be lower, for sure.

Response: Thank you very much for your comment. It is really true that the variability between factors of safety is very high. In the revised manuscript, we reduced the strength of intact materials to account for the smaller fractures, which has been explained in the response to Comment 1. In the recalculation of factors of safety, a lower variability was indeed observed (from 12 to 38) and absolute values were also lower. The result showed that the final factor of safety of the rock slope is 19, which is lower than the previous one (43.5). (Page 24: Figure 12a)

Comment 27: Line 290: again, just a comment. The limitations of this estimation is that it assumes that the base of the model is constituted by strong rock, likely with high coefficient of restitution, and the distribution of the failed mass over this distance is not considered.

Response: Thank you very much for your comment. It is really true that the base of the model is constituted by strong rock, which is represented by a rough rigid wall in PFC. The distribution of the failed mass over the distance is not analysed since this result cannot be proved a statistical significance. The accumulation results vary for 100 different SRM models, which can be verified in Fig. 13. The only thing common is that the final deposit is composed of relatively intact rock blocks and crushed particles, and the blocks pile up above the crushed particles, presenting an inverse grading phenomenon.

Comment 28: Lines 301-303: this sentence is unclear and requires rephrasing.

Response: We are very sorry for our unclear description. In the revised manuscript, we rewrote this sentence as “The factor of safety of the investigated slope is extremely high but reasonable. In the field investigation, weak interlayer and through-going discontinuities are not observed. The non-persistent fractures are very developed, which therefore play a vitally important role in the stability of the investigated slope”. (Page 12: Lines 352-354)

Comment 29: Lines 303-305: I agree with the authors here: rock bridges are multiple orders of magnitude stronger than discontinuities, and this justifies the high FoS. The questions, however, is:

are these estimations accurate and representative of the real situation? Figure 4 shows a rock mass significantly more fractured than the DFNs employed in this study, where the slope is formed by very large, intact blocks.

Response: Thank you very much for your comment. On the basis of our previous results (small fractures are not considered), the factors of safety are accurate and can represent the real situation. This is because we also calculate the factors of safety by the traditional methods (i.e., the ratio of the resisting force to the driving force), which presents the same result as the simulation ones.

The DFNs in Fig. 4 are totally introduced into the simulated slopes, which is reflected by the comparison between Fig. 4 and Fig.7. As for very large and intact blocks you mentioned, maybe you refer to the blocks of the boundary sections located in the bottom and right sides of the slope section. The boundary section won't affect the slope stability, which mainly contributes to overcome boundary effect. In the revised manuscript, we added the description regarding the boundary section as "The bottom and right sides of the slope section were expanded by 10 m as the boundary section, which aims to avoid boundary effect and does not affect the slope stability (Fan et al., 2004)". (Page 7: Lines 220-222)

Comment 30: Figure 1c: a scale and possibly a north arrow is required

Response: Thank you very much for your suggestion. In the revised manuscript, we added the scale and the strike of the slope in Fig. 1c. (Page 17: Figure 1c)

Comment 31: Figure 7: a legend bar (stress) and scales are needed for clarity

Response: Thank you very much for your suggestion. In the revised manuscript, we added the legend bar and scales in Fig. 7 as you suggested. (Page 20: Figure 7)

Comment 32: Figures 8 and 10: the use of an uniform color bar and legend would enhance the comparison of the states depicted by each sub-figure.

Response: Thank you very much for suggestion. It is really true that a uniform color bar and legend makes it convenient to compare different stages in each picture. However, the selected stages show considerable differences of displacements (especially stages in Fig. 8), a uniform color bar and legend presents potential drawbacks. If a small color bar and legend is adopted, the large displacements will appear the same color (red here), which makes it difficult to distinguish

the displacements of different rock blocks; if a large color bar and legend is used, the initial displacements is difficult to be captured and cannot make the profile of slip surface clear. Therefore, we are afraid that a uniform color bar and legend cannot be realised in Figs. 8 and 10.

Comment 33: Table 4: I recommend using the same order for micro, numerical, and lab parameters: friction, normal, and tangential stiffness.

Response: Thank you very much for your suggestion. The same order for micro, numerical and lab parameters is more beneficial for comparing the results of parameter determination. In the revised manuscript, we changed the order of parameters to ensure they are orderly arranged. (Page 25: Table 4)

We thank you for your valuable comments and suggestions. These comments are all valuable and helpful in revising and improving our paper, as well as in guiding the significance of our research.

Relevant references:

Bonilla-Sierra, V., Scholtès, L., Donz é F. V., and Elmouttie, M. K.: Rock slope stability analysis using photogrammetric data and DFN–DEM modeling, *Acta Geotech.*, 10, 497–511, 2015.

Chen, J. P., Shi, B. F., and Wang, Q.: Study on the dominant orientations of random fractures of fractured rock mass, *Chinese Journal of Rock Mechanics and Engineering*, 24, 241–245, 2005.

Damjanac, B., Cundall, P.: Application of distinct element methods to simulation of hydraulic fracturing in naturally fractured reservoirs, *Comput. Geotech.*, 71, 283-294, 2016.

Elmo, D., Stead, D., Eberhardt, E., and Vyazmensky, A.: Applications of finite/discrete element modeling to rock engineering problems, *Int. J. Geomech.*, 13, 565–580, 2013.

Fan, S. C., Jiao, Y. Y., and Zhao, J.: On modeling of incident boundary for wave propagation in jointed rock masses using discrete element method, *Comput. Geotech.*, 31, 57–66, 2004.

Kulatilake, P. H. S. W. and Wu, T. H.: Estimation of mean trace length of discontinuities, *Rock Mech. Rock Eng.*, 17, 215–232, 1984.

Lajtai, E.Z.: Shear strength of weakness planes in rock, *Int. J. Rock Mech. Min.*, 6, 499–515,

1969b.

Lorig, L. J., Darcel, C., Damjanac, B., Pierce, M., and Billaux, D.: Application of discrete fracture networks in mining and civil geomechanics, *Mining Technology*, 124, 239-254, 2015.

Priest, S. D.: *Discontinuity analysis for rock engineering*, London : Chapman and Hall, 1993.

Pine, R. J., Coggan, J. S., Flynn, Z. N., and Elmo, D.: The development of a new numerical modelling approach for naturally fractured rock masses, *Rock Mech. Rock Eng.*, 39, 395–419, 2006.

Shang, J., West, L. J., Hencher, S. R., Zhao, Z.: Geological discontinuity persistence: Implications and quantification, *Eng. Geol.*, 241, 41-54, 2018.

Terzaghi, K.: Stability of steep slopes on hard unweathered rock, *Géotechnique*, 12, 251–270, 1962.

Zhang, W., Zhao, Q. H., Chen, J. P., Huang, R. Q., and Yuan, X. Q.: Determining the critical slip surface of a fractured rock slope considering preexisting fractures and statistical methodology, *Landslides*, 14, 1253–1263, 2017.

Zhang, W., Fu, R., Tan, C., Ma, Z. F., Zhang, Y., Song, S. Y., Xu, P. H., Wang, S. N., Zhao, Y. P.: Two-dimensional discrepancies in fracture geometric factors and connectivity between field-collected and stochastically modeled DFNs: A case study of sluice foundation rock mass in Datengxia, China, *Rock Mech. Rock Eng.*, 53, 2399–2417, 2020a.

Zhang, W., Lan, Z. G., Ma, Z. F., Tan, C., Que, J. S., Wang, F. Y., Cao, C.: Determination of statistical discontinuity persistence for a rock mass characterized by non-persistent fractures. *Int. J. Rock Mech. Min.*, 126, 104177, 2020b.

Stability evaluation and potential failure process of rock slopes characterized by non-persistent fractures

Wen Zhang¹, Jia Wang¹, Peihua Xu¹, Junqing Lou², Bo Shan², Fengyan Wang³, Chen Cao¹, Xiaoxue Chen¹, Jinsheng Que⁴

5 ¹College of Construction Engineering, Jilin University, Changchun, 130026, China

²Northeast Electric Power Design Institute CO., LTD. of China Power Engineering Consulting Group, Changchun, 130026, China

³College of Geo-Exploration Science and Technology, Jilin University, Changchun, 130026, China

⁴CCB Cost Engineering & Consulting Co., Ltd., Beijing, 100000, China

10 *Correspondence to:* Peihua Xu (peihxu@126.com), Chen Cao (ccao@jlu.edu.cn)

Abstract. Slope failure, which causes destructive damage and fatalities, is extremely common in mountainous areas. Therefore, the stability and potential failure of slopes must be analyzed accurately. For most fractured rock slopes, the complexity and random distribution of structural fractures make the aforementioned analyses considerably challenging for
15 engineers and geologists worldwide. This study aims to solve this problem by proposing a comprehensive approach that combines the discrete fracture network (DFN) modeling technique, synthetic rock mass (SRM) approach, and statistical analysis. Specifically, a real fractured rock slope in Laohuding Quarry in Jixian County is studied to show this comprehensive approach. DFN simulation is performed to generate non-persistent fractures in the cross section of the slope. Subsequently, SRM approach is applied to simulate the slope model using 2D particle flow code software (PFC2D). A
20 stability analysis is carried out based on the improved gravity increase method, emphasizing the effect of stress concentration throughout the formation of the critical slip surface. The collapse, rotation, and fragmentation of blocks and the accumulation distances are evaluated in the potential failure process of the rock slope. 100 slope models generated with different DFN models are used to repeat the aforementioned analyses as the result of a high degree of variability in DFN simulation. The critical slip surface, factor of safety, and accumulation distance are selected by statistical analysis for safety
25 assurance in slope analysis and support.

Keywords. Fractured rock slope, Synthetic rock mass, Statistical analysis, Stability evaluation, Potential failure

1 Introduction

Rockslides are common geological hazards in mountainous areas. This phenomenon seriously threatens human lives and properties worldwide every year. Therefore, the analyses of rock slopes, especially their stability and failure process, are
30 necessary for civil and mining engineering. Generally, rockslides are controlled by discontinuities (such as beddings, faults,

and structural fractures). Discontinuities in rock slopes were formerly assumed in slope analysis as through-going and fully persistent planes. However, many researchers have suggested that discontinuities are generally not fully persistent (Eberhardt et al., 2004; Scavia, 1995; Terzaghi, 1962) and that failure surface is a combination of preexisting non-persistent discontinuities and newly propagated cracks (Brideau et al., 2009; Einstein et al., 1983; Frayssines and Hantz, 2006; Lajtai, 1969a; Zhang et al., 2017). Non-persistent fractures are highly complex and come in various sizes and properties, and their locations and characteristics are difficult to determine. Thus, the influence of non-persistent fractures on slope analysis poses a great challenge (Fan et al., 2015; Wasantha et al., 2014).

Several researchers showed that non-persistent fractures play vital roles in the stability and failure process of fractured rock slopes (Gao et al., 2017; Huang et al., 2015; Jiang et al., 2015; Li et al., 2009; Zhang et al., 2015; Zhou et al., 2017). However, the non-persistent fractures in these works were artificially specified by researchers as having the same sizes and orderly arranged locations. The complexity and random distribution of non-persistent fractures in rock slopes should be considered in reflecting and modeling the stability and failure process of real rock slopes in nature.

According to a major research work on fractured rock masses, the discrete fracture network (DFN) modeling technique maximizes the use of discontinuity data from exposed surfaces and can become the best option for simulating realistic fractured rock masses (Bonilla-Sierra et al., 2015; Chen, 2001; Elmo et al., 2013; Pine et al., 2006). By coupling the DFN technique with continuum, discontinuum, and hybrid modeling approaches, synthetic rock mass (SRM) models can be set up to investigate the mechanical properties of fractured rock masses (Elmo and Stead, 2009; Mas Ivars, 2010; Pierce et al., 2007). SRM approach has been widely used to determine the representative elementary volume size of a fractured rock mass (Esmaili et al., 2010), reproduce rock mass properties and behaviours (Mas Ivars et al., 2011), and simulate fracture propagation in a fractured rock mass (Zhang and Stead, 2014). SRM models have been primarily used to simulate failure and deformation of fractured rock slopes (Bonilla-Sierra et al., 2015; Elmo et al., 2013), simulate hydraulic fracturing in naturally fractured reservoirs (Damjanac and Cundall, 2016), and estimate rock mass strength, fragmentation and micro seismicity in caving mines (Lorig et al., 2017). DFN simulation included in SRM modeling program presents a significant variability, which means numerously possible realizations of 2D fracture systems exist given specified input parameters (Pine et al., 2006; Zhang et al., 2020a). The results of SRM model analyses that incorporate different DFN models may vary significantly (Elmo et al., 2018; Zhang et al., 2012). Therefore, rock slope analyses based on only one DFN model can lead to erroneous results (Elmouttie and Poropat, 2014; Mas Ivars, 2006). A statistical analysis based on a large number of DFN models may reduce the aforementioned errors and provide reasonable results for rock slope analysis and support (Ferrero et al., 2016; Zhang et al., 2013; Zhang et al., 2017).

The current study proposes a comprehensive approach that combines several well-established methods to conduct a stability evaluation and failure process analysis of a fractured rock slope in Tianjin City, China. First, 100 DFN models are generated on the basis of the fractures collected in the field. Second, slope models are constructed using SRM approach. Third, the improved gravity increase method is employed to determine the stability of a single-slope model. Fourth, the potential failure processes of the fractured rock slope models are simulated. Fifth, the final critical slip surface, factor of

65 safety, and accumulation distance are determined on the basis of the statistical analysis of 100 slope models generated with
different DFN models.

2 Study area and data acquisition

2.1 Study area

70 A rock slope in Laohuding Quarry, which is located north of Jixian County, Tianjin, is analyzed in this study (Fig. 1). The
quarry was originally used for mining stromatolites, and this activity seriously damaged vegetation. After the mining area
was closed, many steep slopes with internally developed discontinuities were formed. **These slopes may become rock falls
and pose potential threats to people and nearby equipment. Whether rock slide will happen requires calculating and
evaluating.**

75 **The Laohuding Quarry area is characterized by the low-mountain terrain, which is higher in the north than in the south.
The highest and lowest altitudes of the quarry area are 160 m and 60 m, with a relative elevation of 100 m. A majority of
monoclinical mountains striking south–north exist in this area. The average slopes of the mountains in the east and west of the
quarry area are 25 °and 30 °, respectively (Fig. 1b).**

80 This region has a continental climate with an average annual precipitation of 770.20 mm. The flood season is from June
to August, and it accounts for 77.3 % of the annual precipitation. During this period, slope failures are frequently triggered.
The average annual evaporation is 1867.30 mm, which is 2.42 times the amount of precipitation. These conditions indicate
that the region is arid.

85 The lithology in this area is characterized by limestone of the middle-upper Proterozoic erathem, which exhibits a
powder crystal–mud crystal structure. The limestone is moderately **weathered, and the karst phenomena are scarcely visible
due to low precipitation and groundwater shortage. Faults, folds, bedding planes, shear zones and weak interlayers are not
observed, and thus, this area is tectonically stable. Non-persistent discontinuities are randomly and widely developed in
outcrops (Fig. 1c). Therefore, it is the non-persistent discontinuities (fractures) that control the slope stability and potential
failure process.**

2.2 Data acquisition and DFN generation

90 The investigated rock slope is 20 m high and is oriented at a trend of 200 ° with an approximately vertical angle (Fig. 1c).
Fractures in the exposed surface with trace lengths smaller than 1.5 m are widely distributed and difficult to record.
Therefore, these fracture are not considered when performing fracture data collection for 2D DFN simulation. Nevertheless,
the effect of these fractures on the rock mass strength is considered, which is explained in Sect. 3.1. The characteristics (such
as orientation, trace length, spacing, roughness, aperture, filling, and termination) of fractures with trace lengths larger than
1.5 m were systematically surveyed using the sampling window method (Kulatilake and Wu, 1984). The rectangular
95 sampling window was measured 62 m long and 6m high. Exactly 169 fractures were collected, and the 2D trace map is

shown in Fig. 2. The mechanical properties of the different rock mass structures vary, and thus, an evaluation of the homogeneity of the fractured rock mass was conducted (Zhang et al., 2011). The result shows that this region can be considered as a statistically homogeneous area. **The fractures can be divided into three sets using the method proposed by Chen et al. (2005), as shown in Figure 3.** Fractures in set 1 with an average orientation of $39.5^\circ/87.3^\circ$ (dip direction/dip angle) are rare. Fractures in sets 2 and 3 with an average orientation of $307.4^\circ/44.7^\circ$ and $110.2^\circ/31.7^\circ$, respectively, host the most fractures and constitute the dominant sets (Table 1). The Fisher constants (K) ranging from 9.1 to 17.1 imply the high dispersion of fracture orientations (Fisher, 1953; Priest, 1993).

The sampling window method features two main limits of orientation bias and trace length bias. The measured trace lengths bias occurs due to the following: (a) only one end of a fracture is measured, (b) both ends of a fracture are measured, and (c) no end of a fracture is measured. The mean value and probability density function (PDF) of the corrected trace lengths for each fracture set can be determined according to the methods proposed by Kulatilake and Wu (1984) (Table 1). **Orientation bias occurs because the fractures with small intersection angles between the fractures and exposed rock surface are more possibly collected in the field than those fractures with large angles (Nie et al., 2020). In the present study, a 2D analysis was performed. The cross section normal to the exposed surface was used to perform the 2D stability analysis and investigate the potential failure mechanism of the rock slope. The dip directions of fractures in set 1 are similar to that of the cross section, implying fractures acted as the surface of separation, which will not influence the results of stability analysis. Therefore, a substantial portion of the fractures of set 1 (fractures intersected by the cross section with an angle smaller than 20°) were artificially deleted prior to the stability analysis.**

We derived the characteristics of the fractures (location, orientation, trace length, and density) in the cross section from those features measured from the exposed surface. Subsequently, the 2D fracture traces were generated using Monte Carlo simulation by synthesizing the aforementioned characteristics (Li et al., 2020). The specific processes are clearly described in the research of Zhang et al. (2017) and are briefly introduced as follows. The locations of the fractures were assumed to follow Poisson's distribution. **We rotate the slope 20° so that the slope strikes in the NS direction and assume the fracture frequency measured along the mean normal vector direction of fracture set i is λ_i , and the acute angle between this direction and NS direction is η_i . The fracture frequency along the line parallel to the strike of the outcrop plane is $\lambda_i \cos \eta_i$ (Priest 1993), and the cross section plane is $\lambda_i \sin \eta_i$. The fracture frequency of the latter is $\tan \eta_i$ times that of the former, and P_{21} (2D fracture intensity) follows this result according to the concept of the integral.** The 2D orientation of a fracture is reflected by its trace gradient k , which can be expressed as $\sin \alpha / \cot \beta$ (where α and β are the dip direction and dip angle of a 3D fracture, respectively). Empirical distribution was followed to generate the 3D fracture orientations based on the fracture orientation frequency, and then k in the cross section can be determined. The results of Zhang et al. (2017) revealed that the mean [$E(ch^2)$] and variance [$V(ch^2)$] values of the trace length square are constant. $E(ch^2)$ and $V(ch^2)$ of the collected fracture traces in the cross section can be determined according to those features on the exposed surface. The rooted numbers result in the trace lengths in the cross section. The cross section of the investigated rock slope was 20 m high, and the smallest mean dip angle of the three fracture sets was 31.7° . Thus, the length of the cross section was 30 m [$20 \times \cot(31.7^\circ)$]. Finally, we used

130 Monte Carlo simulation to merge the aforementioned parameters to generate the 2D DFN model in a 30 m × 20 m cross section.

More than one DFN can be generated on the basis of the aforementioned statistical fracture data. For example, Fig. 4 exhibits four DFNs with the same statistical fracture data, but fracture characteristics, such as locations, dip angles, trace lengths, are different from one another. Therefore, the rock slope analyses based on only one DFN model can lead to wrong results (Mas Ivars, 2006; Xu et al., 2014). To solve this problem, we generated and verified the validity of numerous DFN models by applying the following method. Initially, we intersected the fractures in the exposed surface with lines extending along the dip direction. Doing so produced a series of intersection points for an individual line. Subsequently, we intersected the DFN models using lines extending along the dip direction of the cross section and consequently generated a series of intersection points for an individual network. We compared these two sets of intersection points by using their probability density curves. The DFN models generated in the cross section proved reasonable when the results were identical to one another. Finally, we selected 100 reasonable DFN models to construct different slope models and conduct stability analysis and potential failure process simulation.

3 SRM model for rock slope analysis

SRM approach is used to construct fractured rock slope models. In the present study, the SRM model used was a combination of two well-established models, namely, the bonded-particle model (BPM) in PFC2D and the DFN model (details are available in the research of Pierce et al. (2007)). SRM approach is widely used to reproduce the mechanical properties and behaviours of fractured rock masses, simulate the fracture propagation and brittle failure of fractured rock masses, and perform stability analysis of fractured rock slopes.

3.1 Parameter determination for SRM model

150 The SRM model in PFC2D is defined by many parameters, such as particle contact modulus, particle normal/shear stiffness ratio, and parallel bond modulus. These parameters cannot be directly identified via laboratory and field experiments. Therefore, the parameters of the model should be predetermined according to the macroscopic characteristics of rock slopes. In particular, several numerical tests should be performed to ascertain and quantify the input parameters of the BPM and DFN model. In PFC2D, a material is considered an assemblage of bonded rigid circular particles, and particle size distribution dramatically influences modeling behaviour (Mas Ivars et al., 2011). Therefore, determining the particle size of a numerical specimen remains a challenge. Generally, the ratio between the maximum and minimum radii of particles is 1.66 (Potyondy and Cundall, 2004). A small particle size is indicative of accurate simulation results. However, the number of particles of rock models increases with a decrease in particle size. A large amount of particles will result in a long calculation time and low computational efficiency. In the present study, particles with radii between 0.05 and 0.083 m were finally

160 selected to fill rock models after repeatedly changing the particle size. In that case, the size of particles is small enough for the comparatively reasonable results and the calculation time is acceptable.

The BPM parameters are calibrated against laboratory uniaxial and biaxial compression tests. The specimens (the height-to-diameter ratio is 2:1) for the numerical uniaxial and biaxial compression tests are set up to reproduce the macro-properties of real rock materials, such as uniaxial compressive strength (σ_c), elastic modulus (E), Poisson's ratio, friction angle, and cohesion obtained in laboratory tests. Different macro-properties are influenced by different parameters in PFC2D. Specifically, E is mainly controlled by several parameters, including particle contact modulus (E_c), particle normal/shear stiffness ratio (k_n/k_s), parallel bond modulus (E_b), and parallel bond normal/shear stiffness ratio (k_{nb}/k_{sb}); Poisson's ratio is influenced by k_n/k_s and k_{nb}/k_{sb} ; σ_c is influenced by tensile strength and cohesion of parallel bonds. Finally, the coefficient of friction is calibrated using the results of biaxial tests (Bahaaddini et al., 2013). The values of the aforementioned parameters are empirically assigned in advance, and then the numerical uniaxial and biaxial compression tests are carried out. When the macro-properties of the numerical tests correspond to the results from the laboratory tests, the parameters are considered reasonable. Otherwise, the parameters are adjusted until the rock specimens have the same macro-properties as real rock materials (Park and Song, 2009; Yang et al., 2006). The calibrated parameters of particles and bonds are listed in Table 2. The macro-properties of the rock specimens for the numerical tests and those of the real rock materials for the laboratory tests are listed in Table 3.

It should be noted that parameters in Table 2 are representations of intact rock materials in PFC2D. However, fractures with trace lengths smaller than 1.5 m were disregarded in the collection of fracture data, but these clearly represent a weakness. Considering the effect of these fractures on strength of the intact rock material make a significant difference to the following stability analysis. In the present study, the combination of intact rock mass and these small fractures is considered as the equivalent rock mass. Obtaining the equivalent shear strength of the equivalent rock mass is extremely important since the rock mass failure is generally promoted by the reduction of the shear strength of rock mass (i.e., the shear strength reduction method). An equivalent shear strength calculation was developed based on the Mohr-Coulomb criterion (Lajtai, 1969b; Shang et al., 2018), as expressed by the following equation:

$$\tau = c_e + \sigma \tan \varphi_e = [K_L \cdot c_f + (1 - K_L) \cdot c_R] + \sigma [K_L \cdot \tan \varphi_f + (1 - K_L) \cdot \tan \varphi_R] \quad (1)$$

185 where τ and σ represent equivalent shear strength of the equivalent rock mass and normal stress; c_e and φ_e are the equivalent cohesion and friction angle of equivalent rock mass; c_f and φ_f are the cohesion and friction angle of fractures; c_R and φ_R are the cohesion and friction angle of intact rock mass; K_L is the linear persistence.

The values of c_R , φ_R and φ_f are 12.25, 25, and 18, which are listed in Tables 2 and 3. Field investigation demonstrated that no fillings existed in fractures, implying the cohesion of fractures is equal to zero (i.e., $c_f = 0$). The linear persistence is defined as the ratio of fracture trace lengths and the total length of coplanar given line (Shang et al., 2018; Zhang et al., 2020b). In the present study, several lines with different directions are set in the exposed surface and then the linear persistence is measured. The average linear persistence is considered as the final linear persistence of the equivalent rock

mass, whose value is around 50%. Subsequently, substituting aforementioned parameters into Eq. (1), we can deduce that the shear strength of the equivalent rock mass is slightly larger than half of intact rock mass. Nevertheless, Eq. (1) tends to overestimate the shear strength of equivalent rock mass; thus, the shear strength of the equivalent rock mass is assumed as half of intact rock mass. This assumption is beneficial to the equivalent reduction of relative parameters of intact rock mass in PFC2D; simultaneously, a smaller strength of equivalent rock mass contributes to a relatively small factor of safety, which is more conservative and favourable for engineering projects.

The shear strength of rock materials is controlled by three parameters (including tensile strength of parallel bond, cohesion of parallel bond and friction coefficient of particles) in PFC2D (Bonilla-Sierra et al., 2015). Therefore, these three parameters are synchronously reduced by half while other parameters are kept constant. Specifically, the values of the tensile strength and cohesion of parallel bond and friction coefficient of particles are 12.5MPa, 12.5MPa and 0.35, respectively. By this way, the effect of small fractures are considered in the generation of intact rock mass. Equivalent parameters of the equivalent rock material are obtained and adopted in the generation of SRM model.

In PFC2D, a smooth joint (SJ) model is commonly adopted to generate fractures. In this model, two particles that lie on the opposite sides of the intended fracture plane can overlap and *interpenetrate* each other instead of moving along their perimeters, thereby reproducing the real physical and mechanical properties of fractures (Bahaaddini et al., 2013). The SJ parameters are normal stiffness (\bar{k}_{nj}), shear stiffness (\bar{k}_{sj}), and coefficient of friction (μ_j). To determine these parameters, we built a numerical specimen (with a width-to-height ratio of 1:1) for the direct shear tests and normal deformability tests to simulate macro-properties, including shear stiffness, normal stiffness, and friction angle. The SJ parameters can be obtained as long as the test results approximate those of the laboratory tests. Specifically, \bar{k}_{nj} was obtained by the numerical normal deformability tests; \bar{k}_{sj} and μ_j were determined by the numerical direct shear test. Table 4 lists the values of the SJ parameters and the results of the normal deformability and direct shear tests of the numerical and laboratory tests. The specific calibration procedures are complex and are thus not introduced in this paper in detail. Additional details about the calibration can be found in the works of Bahaaddini et al. (2013), Cheung et al. (2013), and Duan et al. (2016).

3.2 Model generation

The investigated rock slope with a relatively low height is located on a ground surface with a relatively flat terrain. The study area is dry, crustal movement is not obvious, and no active fault exists nearby (Sect. 2.1). Thus, the effects of ground stress, water, and earthquake on the slope analysis were not considered in the current work.

The size of the slope section is 20 m (height) \times 30 m (length). The bottom and right sides of the slope section were expanded by 10 m as the boundary section, which aims to avoid boundary effect and does not affect the slope stability (Fan et al., 2004). Ultimately, the size of the SRM model was determined to be 30 m (height) \times 40 m (length) (Fig. 5). The upper boundary of the model was free. Moreover, the left, right, and bottom boundaries were assumed to be smooth rigid walls.

The particles with the same radii (0.05 to 0.083 m) as those reported in Sect. 3.1 were applied to fill the 20 m × 30 m slope section. Considering the small effect of boundary section on the slope analysis, we filled the boundary section with particles with larger radii (0.1 to 0.15 m) to improve computational efficiency (Fig. 5). A total of 48,947 particles were generated, and the parameters presented in Table 2 were adopted for the bonds and rock particles. **Notably, the values of three shear strength parameters (including tensile strength and cohesion of parallel bond and friction coefficient of particles) has been reduced by half according to Sect. 3.1.**

Gravity was applied to the model, and the model was calculated (cycled) until the particle assemblage reached an equilibrium state (i.e., the unbalanced forces reached the required standard of 10^{-6}). Then, **an embedded scripting language in PFC, i.e., FISH, is used to write user-defined functions for extending the functionality or adding user-defined features in PFC. In the present study, we used the FISH functions to add the DFN into the model of the slope section by reading the location data of fractures. Subsequently, the SRM model composed of the BPM and DFN is established (Fig. 5, with the DFN in Fig. 4a as an example).** The SJ parameters presented in Table 4 were adopted for the fractures. **This process ignored the stress concentration at the tips of the structural fractures generated by tectonic stress, which was considered reasonable in this study since the investigated slope is characterized by the low stress conditions and the stress concentration was intensely reduced after the long-term stability of the rock slope.**

The slope was formed within one operation. Therefore, the left boundary (smooth rigid wall) was removed to simulate a one-time excavation of the slope.

4 Stability analysis

4.1 Determining the factor of safety

To trigger instability, an improved gravity increase method is used in this study. The improved gravity increase method was proposed by Meng et al. (2015). This method leads to the failure of a slope in PFC2D by slowly increasing gravity acceleration and reducing the friction coefficient of particles while keeping other parameters constant. **Notably, the amplitude of reduction of the friction coefficient is the same as that of the increase in gravity acceleration. In this way, the resisting force can be fixed and therefore the factor of safety is directly reflected by the driving force.** When the slope model is in a limit equilibrium state, i.e., fractures in the slope are propagated and coalesced until a through-going slip surface (i.e., the critical slip surface) is initially formed, the factor of safety F can be defined as the ratio of the gravity acceleration in the limit equilibrium state (g') to that in the initial state (g), i.e., $F = g' / g$. Taking the model in Fig. 5 as an example, we calculate the factor of safety by using the calculation procedure shown in Fig. 6. The simulation results indicate that the factor of safety of the slope model using the improved gravity increase method is 1.2. Additional details on the factor of safety can be found in Sect. 7 of this paper.

4.2 Initiation and propagation of fractures

255 When the factor of safety is determined, the critical slip surface is simultaneously obtained. To get an in-depth understanding of the fracture propagation mechanism, the propagation process of fractures and the evolution of force chains during the formation of the critical slip surface are recorded (Fig. 7). The force magnitude is proportional to the thickness of the line in the force chain plots (lower right corner of Fig. 7), in which the blue and green lines denote compressive and tensile forces, respectively. The color of the line segments is obvious in the region where the stress concentration is strong.

260 Non-homogeneous stresses are distributed throughout the slope owing to the heterogeneity of the slope model. After 2,000 time steps, the compressive stress, which slowly increases from top to bottom under the action of gravity, is initially distributed throughout the slope. The tensile stress exists only in the tips of the fractures (Fig. 7a). Then, the degree of tensile stress concentration increases at the fracture endpoints (Fig. 7b). The fractures (black lines surrounded by a pink circle in Fig. 7) propagate from the tips of the original fractures (red lines) where the tensile stress is concentrated (Figs. 7a and 7b). After

265 the initiation of fracture propagation, the tensile stress (green markings) at the tips of the original fractures dissipates (lighter green markings). A new tensile stress concentration is found at the tips of the propagated fractures, as shown in the force chain plots in Figs. 7b and 7c. The propagated fractures continuously expand downward to the tips of the neighbouring fractures (or rock surface) accompanied by the concentration and release of tensile stress. The orientation of the yellow arrows in Fig. 7 corresponds to the fracture propagation direction. Finally, a decrease in forces, especially the compressive

270 forces (lighter color) throughout the slope, is observed; furthermore, a through-going surface, i.e., the critical slip surface, is formed when the propagated fractures arrive one after another to the tip of the original fractures (Fig. 7d).

5 Potential failure and accumulation process

According to the aforementioned results of stability analysis, the factor of safety is extremely high such that the investigated rock slope is highly stable. Nonetheless, the potential failure and the accumulation process are simulated in the present study

275 to obtain good knowledge of the failure mechanism of fractured rock slopes and provide references for similar slope projects. To maintain coherence of analysis, we use the model in Fig. 5 as an example. Section 4 presents an analysis of the formation process of the critical slip surface of the gravity-increased model. Subsequently, another round of analysis is performed to determine the failure process after forming the critical slip surface.

Figure 8 presents the displacement field images of the slope model in different time steps. In the displacement field

280 plots, particles are colored according to their relative displacement magnitude. Figure 8a, which corresponds to Fig. 7d, represents the displacement field of particles when the critical slip surface is initially formed. The displacement field image indicates the occurrence of a small deformation in the **failed mass** above the critical slip surface; the bedrock remains stable without a distinguished gap with the **failed mass**. The displacements of the **failed mass** continuously increase, and the largest displacement of the particles (red particles in Fig. 8b) is nearly 0.2 m, which indicates the aggravation of rock failure (Fig.

285 8b). After 60000 time steps, the **failed mass** is slowly fractured into many rock blocks along the non-persistent fractures (Fig.

8c). The displacement and size of these blocks vary from one another. The block fragmentation is apparent near the critical slip surface because of the newly propagated fractures, whereas most of the rock blocks far from the critical slip surface remain intact (Fig. 8d). Ultimately, the **failed mass** is completely separated from the bedrock (Fig. 8d).

As soon as the **failed mass** is detached from the bedrock, a large displacement and movement of blocks occurs. To
290 reflect the actual failure and accumulation process of rock slopes in nature, the PFC2D procedure should be manually interrupted to make corresponding adjustments (when the time steps are 80,000, which correspond to Fig. 8d). First, the particles in the bedrock are deleted to improve computational efficiency, and the critical slip surface is replaced with a rough rigid wall. The frictional properties of the rigid wall are the same as those of the propagated fractures. Then, the DFN model is removed, and the body force in the model is initialized to avoid splitting caused by the release of stress. Finally, the
295 gravity acceleration is restored to 10.0, which corresponds to natural conditions. Figure 9 presents the computed results. In the figure, the blue sections denote the assemblage of rock particles from a macroscopic level while the red lines represent the bonds (contacts) between particles. For a convenient description, we numbered several rock blocks from 1 to 6.

In Fig. 9a (5×10^4 time steps), except for block 2, the blocks rotate under inertia force and gravity and are separated from one another. The blocks near the slip surface are disintegrated into numerous sub-blocks, and even crushed particles. Rock
300 blocks 1, 3, 4, and 5 rotate counterclockwise by approximately 60° , 30° , 260° , and 40° , respectively; whereas block 6 rotates clockwise by 75° (Fig. 9b) when the time steps are 2×10^5 . Block 6 initially crashes to the ground, and the collision results in the bond breakage between particle blocks (red segment in Fig. 9c). Block 6 is divided into two sub-blocks and some crushed particles. Blocks 4, 5, and 2 successively crash to the ground one after another but their shapes are kept intact, whereas block 3 is split owing to the collision with block 6, as shown in Figs. 9c and 9d. As soon as all crushed particles and
305 blocks fall to the ground or the critical slip surface, the blocks and particles slide or roll forward as a whole and are accompanied by a fragmentation of the block edges (Fig. 9e). Figure 9f presents the final **morphology** of the rock model. The final deposit is composed of relatively intact rock blocks and crushed particles, and the blocks pile up above the crushed particles, presenting an inverse grading phenomenon. We also record the final accumulation distance, which is represented by the farthest reach distance of intact blocks (bonds exist in particles in these blocks). The final accumulation distance of
310 the rock slope model shown in Fig. 5 is 28 m.

6 Statistical analysis

The slope analysis in Sects. 4 and 5 are based on a SRM model with one DFN model. However, as mentioned in Sect. 2, numerous DFN models can be generated because of the variability of DFN simulation, and the stability analysis of only one SRM model may lead to erroneous results. In the present study, 100 SRM models on the basis of the different DFN models
315 (generated in Sect. 2), are built to conduct the aforementioned analysis. In particular, the critical slip surfaces and safety factors of these models are calculated using the improved gravity increase method following the calculation procedures in Figure 6. Then, the method mentioned in Sect. 5 is employed to simulate the potential failure and accumulation process.

The factors of safety and the critical slip surfaces of the 100 slope models based on 100 different DFN models significantly vary. For example, Figure 10 exhibits the critical slip surfaces of the SRM models based on DFN models shown in Fig. 4. According to the results, the locations and shapes of the four critical slip surfaces significantly vary, although they all extend along the non-persistent fractures. The factors of safety of these models are 12, 15, 21, and 17.

Figure 11 illustrates the critical slip surfaces of the 100 SRM models on the basis of 100 different DFN models. Figs. 12a and 12b present the factors of safety of the 100 models, ranging from 12 to 38. Therefore, the variability of the simulation results should be emphasized in the stability evaluation of fractured rock slopes. The outcome that considers numerous model calculations may lead to a rational result. In the present study, a statistical analysis method is applied to solve this problem. The final critical slip surface and factor of safety are attributed to conservative considerations. The potential critical slip surface constitutes a large failed mass (Fig. 11). The final critical slip surface covers over 90 % of the failed mass to guarantee safety in the rockslide analysis and support. Additional information on the critical slip surface can be found in the research of Zhang et al. (2017). Critical slip surfaces are supposed to have an arc-shaped geometry that differs from their actual linear or broken line morphologies. Arc morphology is easily defined and is convenient for practical engineering designs. F_s is the final factor of safety of the rock slope when the F values of the other 90 models are greater than F_s . The result shows that the final factor of safety of the rock slope is 19.

Similarly, the results of the potential failure and accumulation process vary. Figure 13 presents the final accumulation states of the models shown in Fig. 10. The plots indicate that the sizes and quantities of the fractured blocks, as well as the rotating degrees, are significantly different. The final accumulation distances of the models are 28, 34, 35, and 40 m.

Finally, the different accumulation distances, with the minimum value of 15 m and the maximum value of 96 m, of the 100 SRM models based on 100 different DFN models are obtained (Fig. 12c). The potential failure and accumulation process based on one SRM model may obtain erroneous results. A statistical analysis method is also applied to solve this problem. To guarantee safety in the rock slope analysis, we attribute the final accumulation distance to conservative considerations. In particular, when the distance values of the other 90 models are lower than a certain value, then the value is the final accumulation distance (D_a) of the rockslide. Therefore, the final accumulation distance is 87 m.

7 Discussion

Slope failure is a 3D stability problem. Thus, constructing a 3D SRM model for stability evaluation and failure process analysis is highly convincing and accurate. A 3D SRM model also combines rock masses in the BPM with DFN model. However, the quantity of rock particles in a 3D slope is extremely large to conduct an effective calculation in PFC. In addition, the factor of safety obtained by 3D analysis is generally higher than that in 2D analysis. Given that many theories and technologies cannot be established and that their adoption cannot perfectly reflect rock masses at present, the accuracy of analyses may not satisfy engineering project requirements. Moreover, deriving a high factor of safety is sometimes unfavourable. Accordingly, 2D analysis, which is simple and commonly used in reality, is adopted in the present study for

350 the stability evaluation and potential failure analysis of the investigated slope. The 2D analytical result can be regarded a good reference, and it provides a theoretical and practical basis for future initiatives that utilize 3D analysis.

The factor of safety of the investigated slope is extremely high but reasonable. In the field investigation, weak interlayer and through-going discontinuities are not observed. The non-persistent fractures are very developed, which therefore play a vitally important role in the stability of the investigated slope. The strength of the rock bridges (intact rock) is considerably
355 higher than that of the fractures. Therefore, the obtained factor of safety is extremely high and is thus reasonable. In addition, the effects of water (rainfall) and earthquakes were ignored in the present study. However, the accuracy of the calculation result would increase if rainfall (seepage analysis) and earthquakes (kinetic analysis) are considered. This topic will be the direction of our future research.

The failure process is unlikely to occur in the investigated rock slope unless it is subjected to significant environmental
360 changes, such as earthquakes, rainfall, unloading, or overloading. Nonetheless, the potential failure process is simulated in this study to understand the rockslide mechanism and subsequently provide a good reference for similar slope projects. For example, the size and motion of rock blocks can be utilized to predict risk degree, and the final accumulation of deposits can contribute to hazardous area division. The final arrangement of deposits (a combination of blocks and crushed particles) provides a good explanation for the inverse grading of rock avalanche reported by Cruden and Hungr, (1986), Imre et al.
365 (2010), and Wang et al. (2012).

DFN simulation presents a high degree of variability and may provide erroneous results. A statistical analysis based on numerous SRM models with different DFN models similar to those performed in the present study can reduce errors and provide conservative results for slope support. Finally, although the final results of the factor of safety, critical slip surface, and accumulation distance can guarantee safety in the rockslide analysis and support, they are not the exact values. Statistical
370 analysis provides a new method for deriving an in-depth understanding of solid earth, where specific locations and characteristics of geological materials and structures remain unknown, such as discontinuities, especially for small-scale non-persistent fractures. Meanwhile, new theories and technologies are required to obtain precise forecasts with respect to the range values characterized by statistical methods.

8 conclusion

375 The present study combines several methods, namely, DFN simulation, SRM approach, and statistical analysis, to conduct stability evaluation and potential failure process analysis of a fractured rock slope in Laohuding Quarry in Jixian County, Tianjin. The SRM technique is utilized to generate a slope model with non-persistent fractures in the form of a DFN. The factor of safety is determined on the basis of the improved gravity increase method. The formation of a critical slip surface is also investigated. The potential failure and accumulation processes are simulated to provide a reference for similar slope
380 projects. Numerous slope models are calculated, and the final results of the safety factor, critical slip surface, and accumulation distance are determined by statistical analysis. The major findings are summarized as follows.

(1) The slope model with non-persistent fractures can be effectively constructed on the basis of SRM technology. The instability of the slope model can be attained by combining the improved gravity increase method or the strength reduction method, thereby obtaining the safety factor and critical slip surface. An innovative formula to calculate the safety factor is proposed by considering stress concentration and the calculation principle of PFC2D.

(2) Fracture propagation is closely related to stress concentration. Fractures initially propagate from the tips of the original fractures where the tensile stress is concentrated. Then, the stress is released, and a new stress concentration occurs at the tip of the propagated fractures when the fracture propagates downward to the neighbouring fractures. The critical slip surface is formed by the coalescence of preexisting fractures and newly propagated fractures.

(3) In the initiation of failure, the failed mass is fractured into rock blocks along the preexisting fractures. Then, most blocks rotate and collapse under inertia force and gravity. Several blocks are split into sub-blocks owing to the collision between the blocks and the ground. The final deposit is composed of intact blocks and crushed particles, presenting inverse grading phenomena.

(4) The critical slip surfaces, factors of safety, and accumulation distances of the slope models with different DFN models vary. Therefore, the final outcome is obtained by statistical analysis. It ensures engineering safety for rockslide analysis and support. The factor of safety (reserve) of the studied rock slope is determined to be 1.9. The critical slip surface is confirmed, as shown in Fig. 11. The final accumulation distance is 87 m.

Data availability. The data from the research findings cannot be shared now, because these data are also part of the future research.

Author contributions. WZ initiated this research, analysed the simulation results, and revised the manuscript. JW wrote software code and wrote this paper. PX, JL and BS conducted field investigation and recorded field data. FW and CC dealt with the field data. XC and JQ guided and collated the software code.

Competing interests. The authors declare that they have no conflict of interest.

Acknowledgements. This work was supported by the National Natural Science Foundation of China (grant nos. 41877220 and 41472243), the National Natural Key Science Program Foundation (grant no. 41330636), the National Key Research and Development Plan (grant no. 2017YFC1501000), and the Science and Technology Project Plan of Northeast Electric Power Company (grant no. K2018N-19).

Financial support. This research has been supported by the National Natural Science Foundation of China (grant nos. 41877220 and 41472243), the National Natural Key Science Program Foundation (grant no. 41330636), the National Key Research and Development Plan (grant no. 2017YFC1501000), and the Science and Technology Project Plan of Northeast Electric Power Company (grant no. K2018N-19).

References

- Brideau, M., Yan, M., and Stead, D.: The role of tectonic damage and brittle rock fracture in the development of large rock slope failures, *Geomorphology*, 103, 30–49, 2009.
- 415 Bahaaddini, M., Sharrock, G., and Hebblewhite, B. K.: Numerical investigation of the effect of joint geometrical parameters on the mechanical properties of a non-persistent jointed rock mass under uniaxial compression, *Comput. Geotech.*, 49, 206–225, 2013.
- Bonilla-Sierra, V., Scholtès, L., Donzé F. V., and Elmouttie, M. K.: Rock slope stability analysis using photogrammetric data and DFN–DEM modeling, *Acta Geotech.*, 10, 497–511, 2015.
- 420 Cruden, D. M. and Hungr, O.: The debris of the Frank slide and theories of rockslide-avalanche mobility, *Can. J. Earth Sci.*, 23, 425–432, 1986.
- Chen, J. P.: 3-D network numerical modeling technique for random discontinuities of rock mass, *Chinese Journal of Geotechnical Engineering*, 23, 397–402, 2001.
- Chen, J. P., Shi, B. F., and Wang, Q.: Study on the dominant orientations of random fractures of fractured rock mass, 425 *Chinese Journal of Rock Mechanics and Engineering*, 24, 241–245, 2005.
- Cheung, L. Y. G., O’Sullivan, C., and Coop, M. R.: Discrete element method simulations of analogue reservoir sandstones, *Int. J. Rock Mech. Min.*, 63, 93–103, 2013.
- Damjanac, B., Cundall, P.: Application of distinct element methods to simulation of hydraulic fracturing in naturally fractured reservoirs, *Comput. Geotech.*, 71, 283-294, 2016.**
- 430 Duan, K., Kwok, C. Y., and Pierce, M.: Discrete element method modeling of inherently anisotropic rocks under uniaxial compression loading, *Int. J. Numer. Anal. Met.*, 40, 1150–1183, 2016.
- Einstein, H. H., Veneziano, D., Baecher G. B., and O’Reilly, K. J.: The effect of discontinuity persistence on rock slope stability, *Int. J. Rock Mech. Min.*, 20, 227–236, 1983.
- Eberhardt, D., Stead, D., and Coggan, J. S.: Numerical analysis of initiation and progressive failure in natural rock slopes—the 1991 Randa rockslide, *Int. J. Rock Mech. Min.*, 41, 69–87, 2004.
- 435 Elmo, D. and Stead, D.: An integrated numerical modelling–Discrete Fracture Network approach applied to the characterisation of rock mass strength of naturally fractured pillars, *Rock Mech. Rock Eng.*, 43, 3–19, 2009.
- Elmo, D., Stead, D., Eberhardt, E., and Vyazmensky, A.: Applications of finite/discrete element modeling to rock engineering problems, *Int. J. Geomech.*, 13, 565–580, 2013.
- 440 Elmo, D., Donati, D., and Stead, D.: Challenges in the characterisation of intact rock bridges in rock slopes, *Eng. Geol.*, 245, 81–96, 2018.
- Esmaili, K., Hadjigeorgiou, J., and Grenon, M.: Estimating geometrical and mechanical REV based on synthetic rock mass models at Brunswick Mine, *Int. J. Rock Mech. Min.*, 47, 915–926, 2010.

- Elmoultie, M. K. and Poropat, G. V.: Quasi-Stochastic analysis of uncertainty for modeling structurally controlled failures, 445 *Rock Mech. Rock Eng.*, 47, 519–534, 2014.
- Fisher, R.: Dispersion on a sphere, *Proceedings of the Royal Society of London*, 217, 295–305, 1953.
- Fan, S. C., Jiao, Y. Y., and Zhao, J.: On modeling of incident boundary for wave propagation in jointed rock masses using discrete element method, *Comput. Geotech.*, 31, 57–66, 2004.
- Frayssines, M. and Hantz, D.: Failure mechanisms and triggering factors in calcareous cliffs of the Subalpine Ranges 450 (French Alps), *Eng. Geol.*, 86, 256–270, 2006.
- Fan, X., Kulatilake, P. H. S. W., and Chen, X.: Mechanical behavior of rock-like jointed blocks with multi-non-persistent joints under uniaxial loading: A particle mechanics approach, *Eng. Geol.*, 190, 17–32, 2015.
- Ferrero, A. M., Migliazza, M. R., Pirulli, M., and Umili, G.: Some open issues on rockfall hazard analysis in fractured rock mass: problems and prospects, *Rock Mech. Rock Eng.*, 49, 3615–3629, 2016.
- 455 Gao, W., Dai, S., Xiao, T., and He, T. Y.: Failure process of rock slopes with cracks based on the fracture mechanics method, *Eng. Geol.*, 231, 190–199, 2017.
- Huang, D., Cen, D. F., Ma, G. W., and Huang, R. Q.: Step-path failure of rock slopes with intermittent joints, *Landslides*, 12, 911–926, 2015.
- Imre, B., Laue, J., and Springman, S. M.: Fractal fragmentation of rocks within sturzstroms: insight derived from physical 460 experiments within the ETH geotechnical drum centrifuge, *Granular Matter*, 12, 267–285, 2010.
- Jiang, M. M., Jiang, T., Crosta, G. B., Shi, Z. M., Chen, H., and Zhang, N.: Modeling failure of jointed rock slope with two main joint sets using a novel DEM bond contact model, *Eng. Geol.*, 193, 79–96, 2015.
- Kulatilake, P. H. S. W. and Wu, T. H.: Estimation of mean trace length of discontinuities, *Rock Mech. Rock Eng.*, 17, 215–232, 1984.
- 465 Lajtai, E. Z.: Strength of discontinuous rocks in direct shear, *Géotechnique*, 19, 218–233, 1969a.
- [Lajtai, E.Z.: Shear strength of weakness planes in rock, *Int. J. Rock Mech. Min.*, 6, 499–515, 1969b.](#)
- Li, L. C., Tang, C. A., Zhu, W. C., and Liang, Z. Z.: Numerical analysis of slope stability based on the gravity increase method, *Comput. Geotech.*, 36, 1246–1258, 2009.
- [Li, K. Q., Li, D. Q., Liu, Y.: Meso-scale investigations on the effective thermal conductivity of multi-phase materials using 470 the finite element method, *Int. J. Heat Mass Tran.*, 151, 119383, 2020.](#)
- [Lorig, L. J., Darcel, C., Damjanac, B., Pierce, M., and Billaux, D.: Application of discrete fracture networks in mining and civil geomechanics, *Mining Technology*, 124, 239-254, 2015.](#)
- Mas Ivars, D.: Water inflow into excavations in fractured rock — a three-dimensional hydro-mechanical numerical study, *Int. J. Rock Mech. Min.*, 43, 705–725, 2006.
- 475 Mas Ivars, D. Bonded particle model for jointed rock mass, Ph.D. thesis, Royal Institute of Technology, Sweden, 2010.
- Mas Ivars, D., Pierce, M. E., Darcel, C., Reyes-Montes, J., Potyondy, D. O., Young, R. P., and Cundall, P. A.: The synthetic rock mass approach for jointed rock mass modelling, *Int. J. Rock Mech. Min.*, 48, 219–244, 2011.

- Meng, Y. D., Su, Q. M., Lu, W. P., and Xu, Z.: Research on improved grain flow gravity increase method, *Chinese Journal of Water Resource and Power*, 33, 149–151, 2015.
- 480 Nie, Z. B., Chen, J. P., Zhang, W., Tan, C., Ma, Z. F., Wang, F. Y., Zhang, Y., Que, J. S.: A new method for three-dimensional fracture network modelling for trace data collected in a large sampling window, *Rock Mech. Rock Eng.*, 53, 1145-1161, 2020.
- Priest, S. D.: *Discontinuity analysis for rock engineering*, London: Chapman and Hall, 1993.
- Potyondy, D. O. and Cundall, P. A.: A bonded-particle model for rock, *Int. J. Rock Mech. Min.*, 41, 1329–1364, 2004.
- 485 Pine, R. J., Coggan, J. S., Flynn, Z. N., and Elmo, D.: The development of a new numerical modelling approach for naturally fractured rock masses, *Rock Mech. Rock Eng.*, 39, 395–419, 2006.
- Pierce, M., Cundall, P., Potyondy, D., and Ivars, D. M.: A synthetic rock mass model for jointed rock, in: *Proceedings of First Canada/United States Rock Mechanics Symposium*, Vancouver, 341–349, 2007.
- Park, J. W., and Song, J. J.: Numerical simulation of a shear test on a rock joint using a bonded-particle model, *Int. J. Rock*
- 490 *Mech. Min.*, 46, 1315–1328, 2009.
- Scavia, C.: A method for the study of crack propagation in rock structures, *Géotechnique*, 45, 447–463, 1995.
- Shang, J., West, L. J., Hencher, S. R., Zhao, Z.: *Geological discontinuity persistence: Implications and quantification*, *Eng. Geol.*, 241, 41-54, 2018.
- Terzaghi, K.: Stability of steep slopes on hard unweathered rock, *Géotechnique*, 12, 251–270, 1962.
- 495 Wang, Y. F., Cheng, Q. G., and Zhu, Q.: Inverse grading analysis of deposit from rock avalanches triggered by Wenchuan earthquake, *Chinese Journal of Rock Mechanics and Engineering*, 1089–1106, 2012.
- Wasantha, P. L. P., Ranjith, P. G., Xu, T., Zhao, J., and Yan, Y. L.: A new parameter to describe the persistency of non-persistent joints, *Eng. Geol.*, 181, 71–77, 2014.
- Xu, Q., Chen, J. Y., Li, J., and Yue, H. Y.: A genetic algorithm for locating the multiscale critical slip surface in jointed rock
- 500 mass slopes, *Math. Probl. Eng.*, 2014.
- Yang, B., Jiao, Y., and Lei, S.: A study on the effects of microparameters on macroproperties for specimens created by bonded particles, *Eng. Computation.*, 23, 607–631, 2006.
- Zhang, W., Chen, J. P., Liu, C. H., Ma, J. Q., and Zhang, C.: Application of chi-square test in structural homogeneity dividing of fractured rock mass, *Chinese Journal of Geotechnical Engineering*, 33, 1440–1446, 2011.
- 505 Zhang, W., Chen, J. P., Liu, C., Huang, R., Li. M., and Zhang, Y.: Determination of geometrical and structural representative volume elements at the Baihetan Dam Site, *Rock Mech. Rock Eng.*, 45, 409–419, 2012.
- Zhang, W., Chen, J. P., Zhang, W., Lv, Y., Ma, Y. F., and Xiong, H.: Determination of critical slip surface of fractured rock slopes based on fracture orientation data, *Sci. China. Technol. Sc.*, 56, 1248–1256, 2013.
- Zhang, W., Zhao, Q. H., Chen, J. P., Huang, R. Q., and Yuan, X. Q.: Determining the critical slip surface of a fractured rock
- 510 slope considering preexisting fractures and statistical methodology, *Landslides*, 14, 1253–1263, 2017.

Zhang, W., Fu, R., Tan, C., Ma, Z. F., Zhang, Y., Song, S. Y., Xu, P. H., Wang, S. N., Zhao, Y. P.: Two-dimensional discrepancies in fracture geometric factors and connectivity between field-collected and stochastically modeled DFNs: A case study of sluice foundation rock mass in Datengxia, China, *Rock Mech. Rock Eng.*, 53, 2399–2417, 2020a.

515 Zhang, W., Lan, Z. G., Ma, Z. F., Tan, C., Que, J. S., Wang, F. Y., Cao, C.: Determination of statistical discontinuity persistence for a rock mass characterized by non-persistent fractures. *Int. J. Rock Mech. Min.*, 126, 104177, 2020b.

Zhang, Y. and Stead, D.: Modelling 3D crack propagation in hard rock pillars using a synthetic rock mass approach, *Int. J. Rock Mech. Min.*, 72, 199–213, 2014.

Zhou, Y., Chai, J. F., and Han, G.: Meso numerical study on the failure mechanism on rock slope with bedding intermittent joints, *Engineering Review*, 37, 272–280, 2017.

520 Zhang, K., Cao, P., Meng, J. J., Li, K. H., Fan, W. C.: Modeling the progressive failure of jointed rock slope using fracture mechanics and the strength reduction method, *Rock Mech. Rock Eng.*, 48, 771–785, 2015.

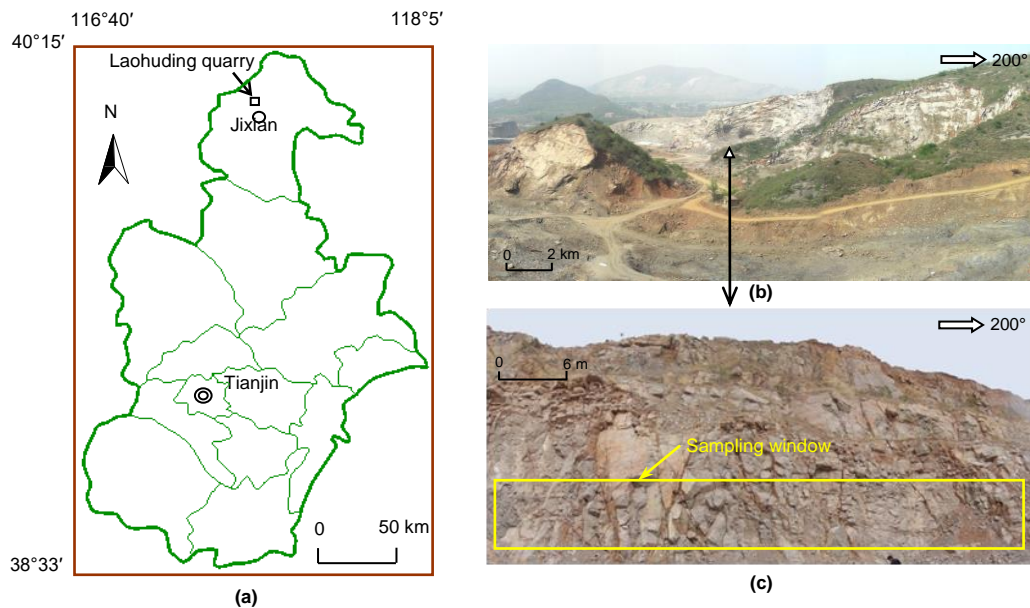
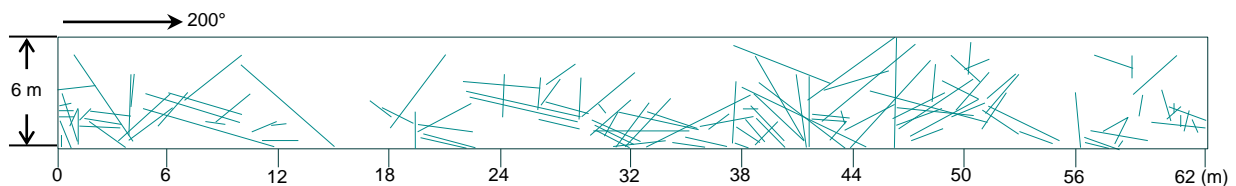


Figure 1: Location of the Laohuding Quarry and investigated rock slope. (a) location of Laohuding Quarry in Tianjin City, China; (b) image of Laohuding Quarry and the location of the investigated rock slope; (c) image of the investigated rock slope.



525

Figure 2: 2D trace chart of collected fractures

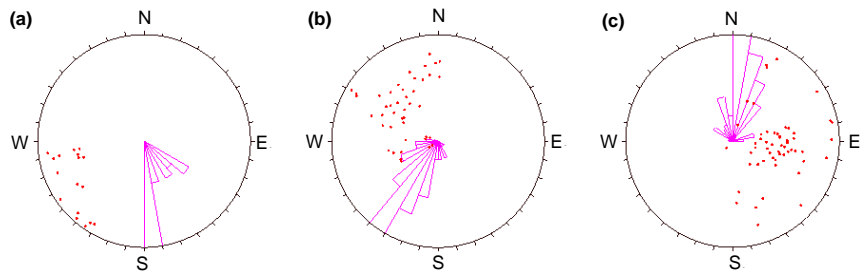
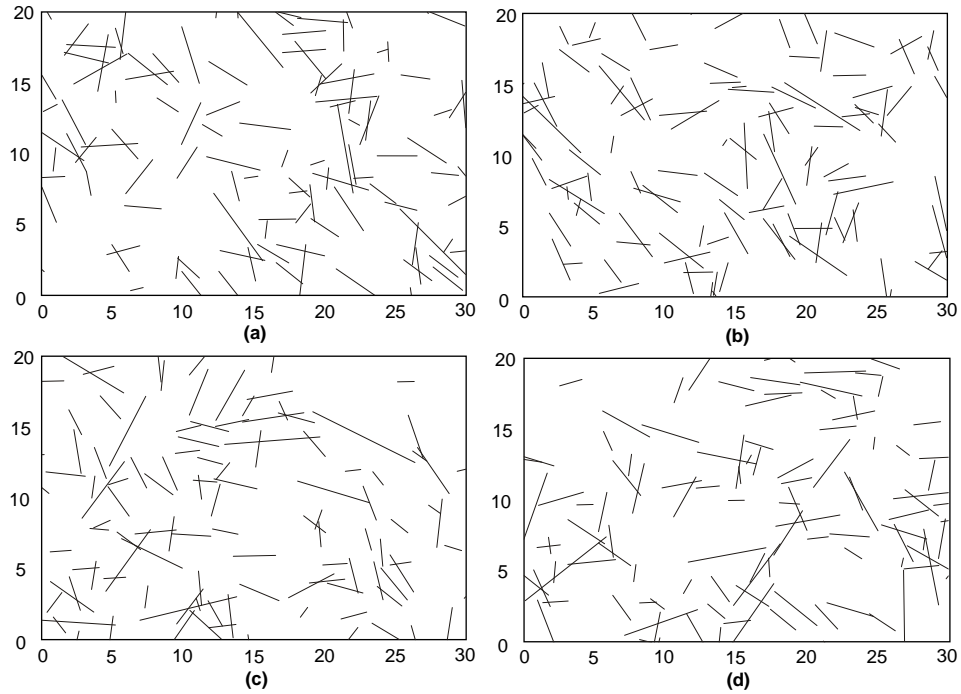


Figure 3: Poles and strike rose diagrams of the fracture sets. (a)–(c) are fracture sets 1, 2, and 3.



530 **Figure 4:** Variability of DFN simulation. (a)–(d) are the DFN models in four simulations. The line segments in the rectangle frame represent the fractures, and the left boundary of the frame represents the exposed surface.

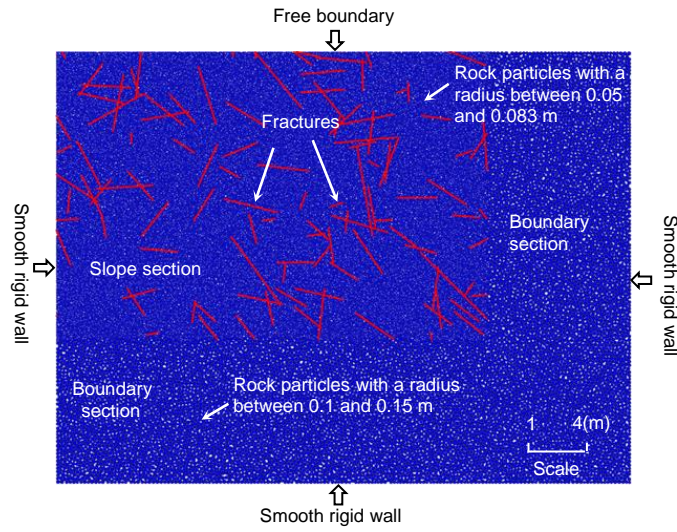
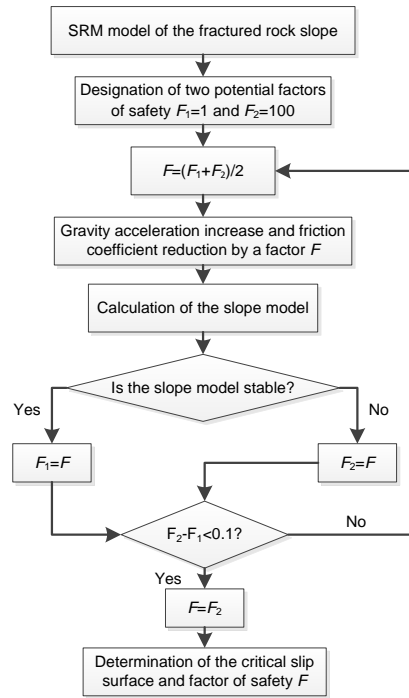
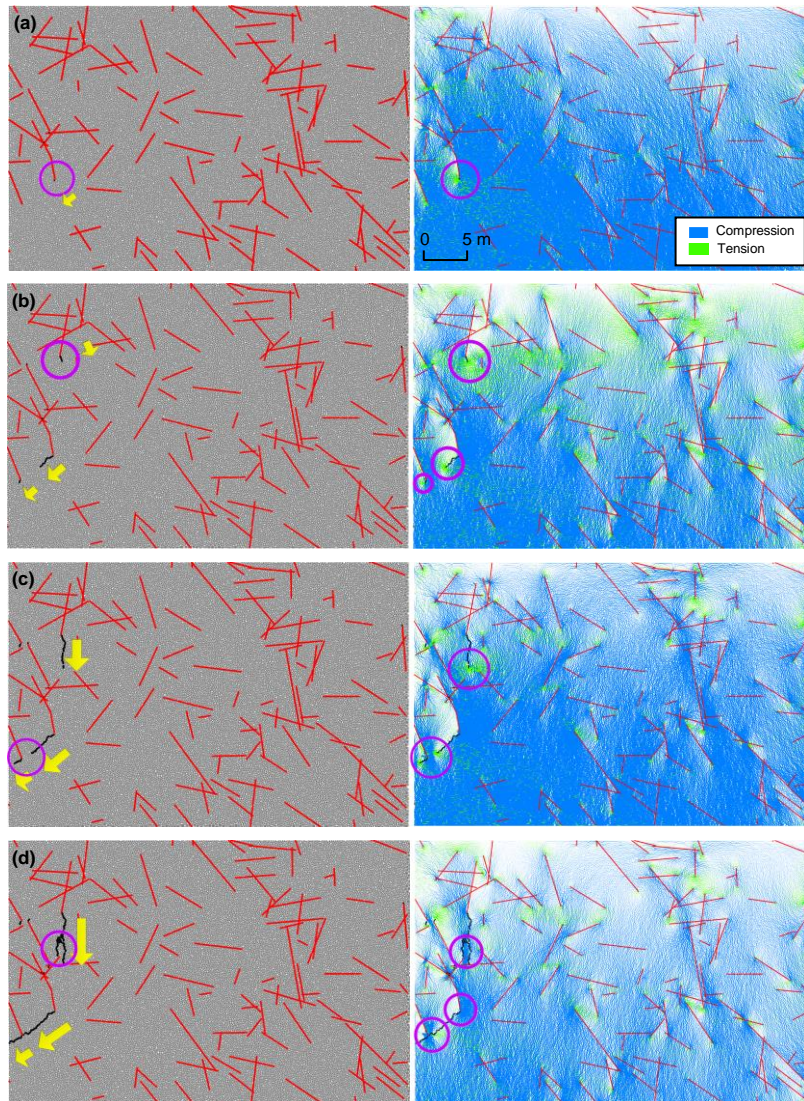


Figure 5: SRM model of the investigated fractured rock slope. The left boundary is the exposed surface.



535 **Figure 6:** Program flow chart for the slope stability analysis.



540 **Figure 7:** Formation process of the critical slip surface (drawings on the left) and force chain plots (drawings on the right). The time steps of (a)–(d) are 2×10^3 , 5×10^3 , 10^4 , and 2×10^4 .

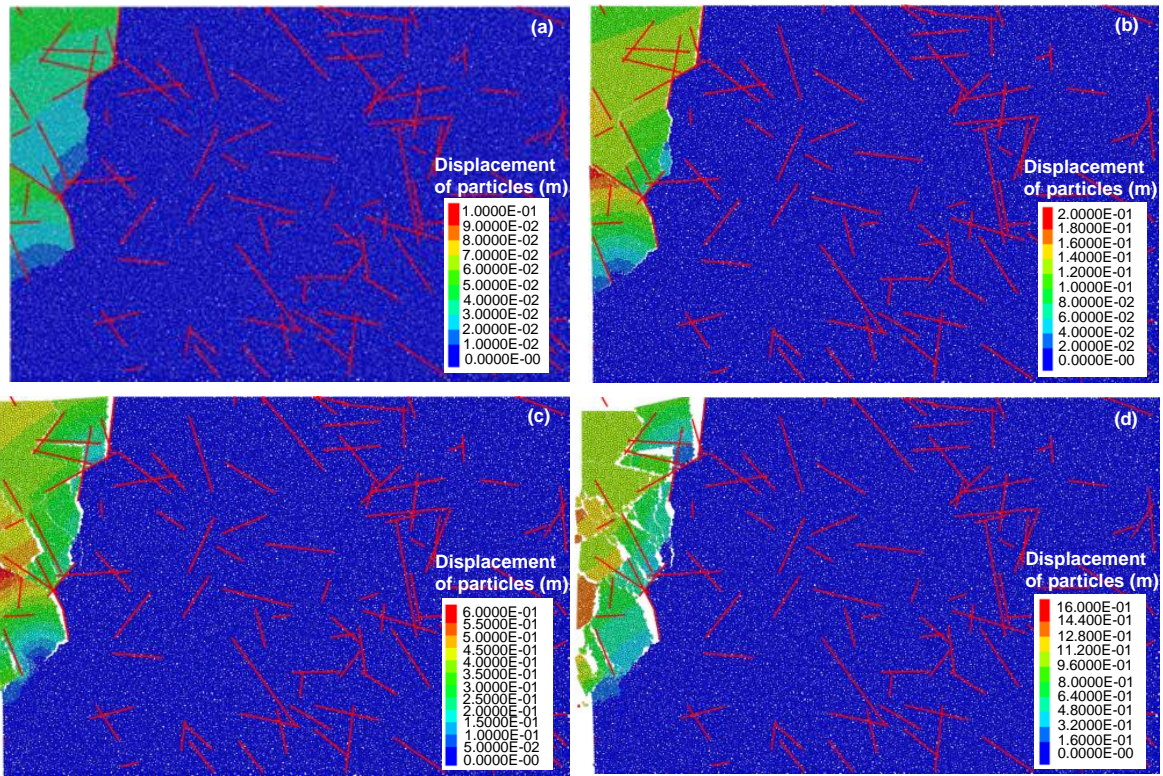
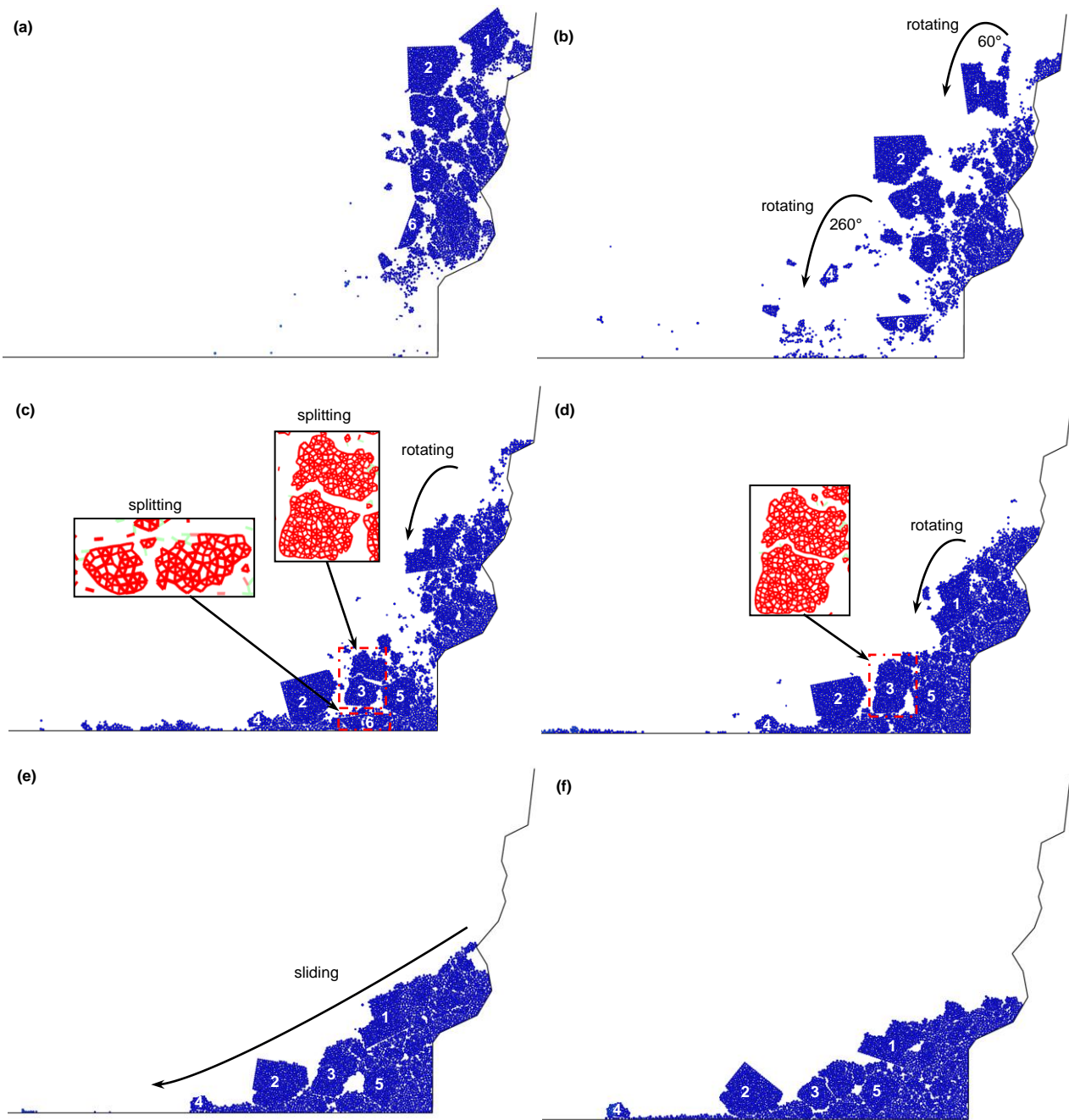


Figure 8: Particle displacement field of the fractured rock slope. The time steps of (a)–(d) are 2×10^4 , 4×10^4 , 6×10^4 , and 8×10^4 .



545 **Figure 9:** Failure and accumulation process of the rock slope. The time steps of (a)–(f) are 5×10^4 , 2×10^5 , 4×10^5 , 8×10^5 , 1.6×10^6 , and 3.2×10^6 .

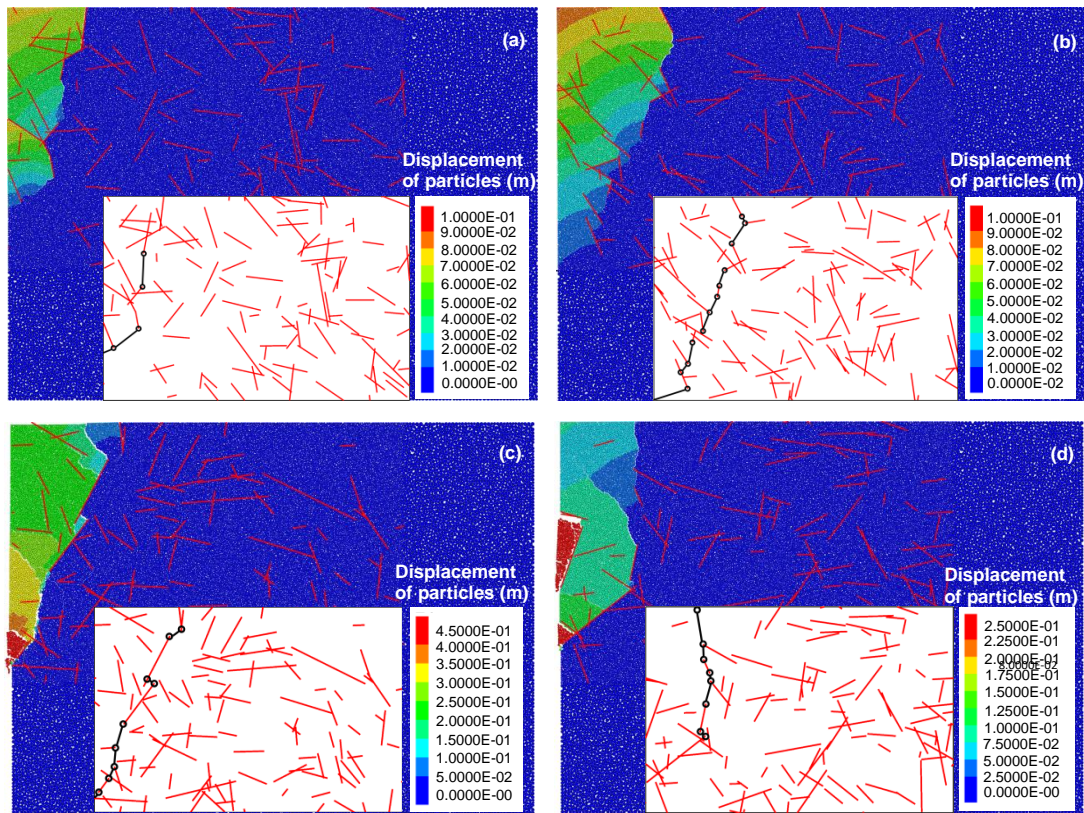


Figure 10: Four different critical slip surfaces of rock slopes with four different DFN models. The factors of safety of (a)–(d) are 12, 15, 21, and 17.

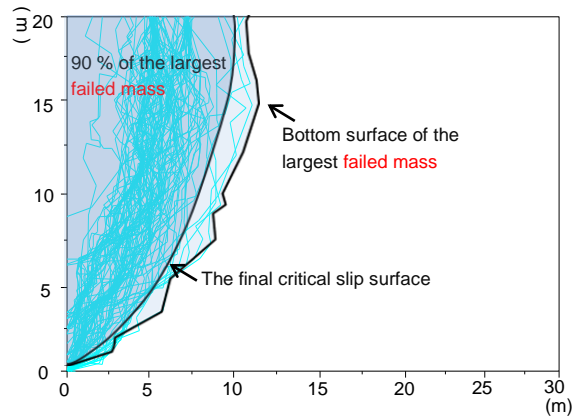


Figure 11: Potential critical slip surfaces of 100 models and the final critical slip surface of the investigated rock slope.

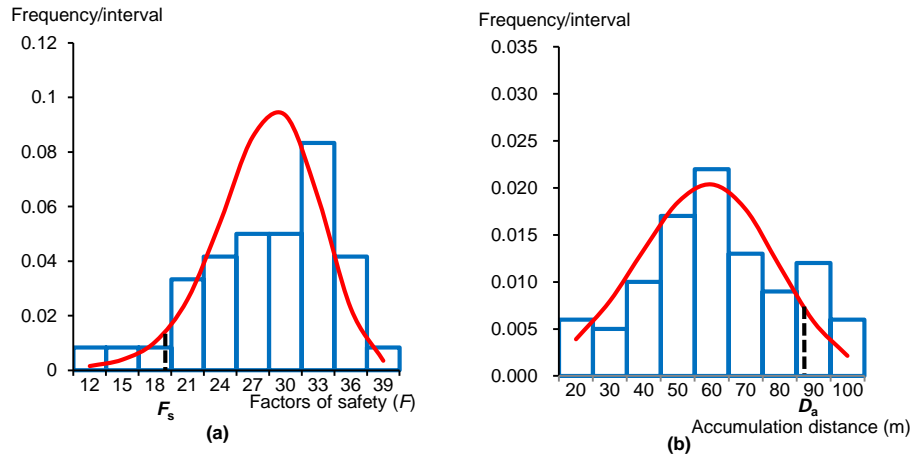
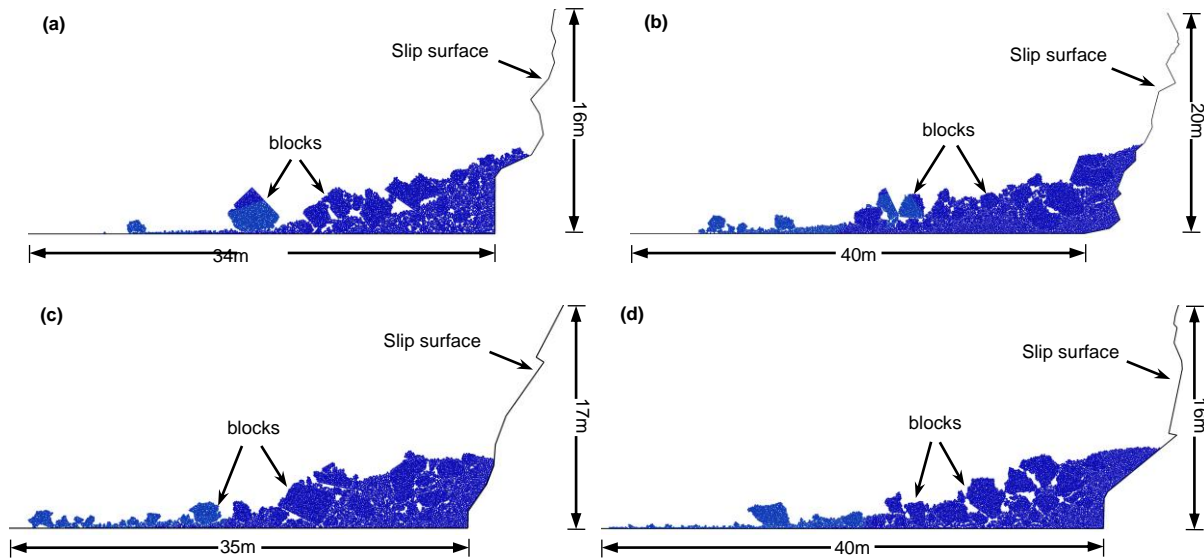


Figure 12: Statistical results of 100 slope models. (a) the final factor of safety F_s of the investigated rock slope; (b) the final accumulation distance D_a of the investigated rock slope.



555

Figure 13: Ultimate accumulation states of rock slopes with different DFN models (partly). The final accumulation distances of (a)–(d) are 28, 34, 35, and 40m.

Table 1: Parameters for discrete fracture network (DFN) simulation.

Fracture set	Fracture number	Dip Direction ($^{\circ}$)	Dip Angle ($^{\circ}$)	Trace length surveyed (m)	Corrected (m)	Std. (m)	Distribution type	R_0	R_1	R_2	$P_{21}(\text{m}^2/\text{m}^2)$	K
1	18	39.5	87.3	2.16	2.42	1.2	Gamma	0.89	0.11	0	0.11	17.1
2	58	307.4	44.7	2.71	2.84	1.7	Log-normal	0.83	0.14	0.03	0.45	10.3
3	93	110.2	31.7	2.33	2.49	1.2	Gamma	0.87	0.13	0	0.63	9.1

Table 2: Values of the BPM parameters.

Particle parameters		Parallel bond parameters	
Particle density (kg/m ³)	2650	E_b (GPa)	23
Minimum particle radius (m)	0.05	k_{nb}/k_{sb}	1.25
Radius ratio	1.66	Normal strength (MPa)	25
Friction coefficient	0.7	Internal friction angle (°)	38
k_n/k_s	1.25	Cohesion (MPa)	25
E_c (GPa)	23	Radius multiplier	1

Table 3: Comparison of macro-properties determined by numerical and laboratory tests.

Macro-parameters	E (Gpa)	Poisson's ratio	Friction angle (°)	Cohesion (Mpa)	σ_c (Mpa)
Numerical tests	35.7	0.23	23	12.68	37.8
Laboratory tests	35	0.24	25	12.25	38.3

Table 4: Calibrated smooth-joint parameters and results of numerical and laboratory tests

Smooth-joint parameters		Test results		
		Parameters	Numerical tests	Laboratory tests
Normal stiffness \bar{k}_{nj} (GPa/m)	10	Normal stiffness (GPa/m)	7.042	7
Shear stiffness \bar{k}_{sj} (GPa/m)	8	Shear stiffness (GPa/m)	3.415	3.4
Coefficient of friction μ_j	0.466	Friction angle (°)	17.87	18